remote sensing

MDPI

Article

Remote Sensing for Agricultural Water Management in Jordan

Jawad T. Al-Bakri [1,*], Guido D'Urso [2], Alfonso Calera [3], Eman Abdalhaq [4], Maha Altarawneh [5] and Armin Margane [6]

[1] Department of Land, Water and Environment, School of Agriculture, The University of Jordan, Amman 11942, Jordan
[2] Department of Agricultural Sciences, University of Naples Federico II, 80055 Portici, Italy
[3] Remote Sensing & GIS Group, Institute for Regional Development, University of Castilla-La Mancha, Campus Universitario SN, 02071 Albacete, Spain
[4] Department of Data Monitoring and Evaluation, Blumont Inc., Amman 11183, Jordan
[5] Water Data, IKMS and GIS Component, USAID-WMI, Amman 11953, Jordan
[6] Water Master Plan & WEAP, GIZ Water Portfolio, MWI, Amman 11181, Jordan
* Correspondence: jbakri@ju.edu.jo; Tel.: +962-79-6169966

Abstract: This study shows how remote sensing methods are used to support and provide means for improving agricultural water management (AWM) in Jordan through detailed mapping of irrigated areas and irrigation water consumption (IWC). Digital processing and classification methods were applied on multi-temporal data of Landsat 8 and Sentinel-2 to derive maps of irrigated areas for the period 2017–2019. Different relationships were developed between the normalized difference vegetation index (NDVI) and the crop coefficient (Kc) to map evapotranspiration (ET). Using ground data, ET maps were transferred to IWC for the whole country. Spatial analysis was then used to delineate hotspots where shifts between ET and groundwater abstraction were observed. Results showed that the applied remote sensing methods provided accurate maps of irrigated areas. The NDVI-Kc relationships were significant, with coefficients of determination (R^2) ranging from 0.89 to 0.93. Subsequently, the ET estimates from the NDVI-Kc relationships were in agreement with remotely sensed ET modeled by SEBAL (NSE = 0.89). In the context of Jordan, results showed that irrigated areas in the country reached 98 thousand ha in 2019, with 64% of this area located in the highlands. The main irrigated crops were vegetables (55%) and fruit trees and olives (40%). The total IWC reached 702 MCM in 2019, constituting 56% of the total water consumption in Jordan, with 375 MCM of this amount being pumped from groundwater, while reported abstraction was only 235 MCM. The study identified the hotspots where illegal abstraction or incorrect metering of groundwater existed. Furthermore, it emphasized the roles of remote sensing in AWM, as it provided updated figures on groundwater abstraction and forecasts for future IWC, which would reach 986 MCM in 2050. Therefore, the approach of ET and IWC mapping would be highly recommended to map ET and to provide estimates of present and future IWC.

Keywords: irrigation; remote sensing; NDVI-Kc; ET; Jordan; water management

Citation: Al-Bakri, J.T.; D'Urso, G.; Calera, A.; Abdalhaq, E.; Altarawneh, M.; Margane, A. Remote Sensing for Agricultural Water Management in Jordan. *Remote Sens.* **2023**, *15*, 235. https://doi.org/10.3390/rs15010235

Academic Editor: Won-Ho Nam

Received: 29 November 2022
Revised: 25 December 2022
Accepted: 29 December 2022
Published: 31 December 2022

1. Introduction

Agricultural water management (AWM) includes the management of water used in crop production (both rainfed and irrigated), livestock, and inland fisheries to sustain food production, while preserving natural resources [1,2]. Due to world population growth, it is anticipated that in the next few decades, the agricultural sector will remain the dominant user of water [3]. This calls for improved AWM that goes beyond the improvement of irrigation system efficiency at farm level towards the assessment and monitoring of large-scale irrigation schemes [4]. Improved AWM on a large scale can be achieved by the adoption of innovative approaches and interventions, supported by effective governance and strong institutions that employ different tools to monitor agricultural water use. The

technological developments of remote sensors, with improved spatial and/or temporal resolution, provide the opportunity to use remote sensing (RS) tools for monitoring and assessment of agricultural water use. This can be achieved by mapping agricultural crops and irrigation water consumption (IWC) and hence assessing water withdrawal for crop irrigation. The use of artificial intelligence algorithms to develop digital image classification methods provides cost-effective and accurate means to derive maps of irrigated crops [5,6]. Analysis of these maps, in addition to ground data, within a geographic information system (GIS) provides important information on levels of agricultural water consumption in relation to water supply. Furthermore, it can show hotspots where water consumption is high and periods when water demand is at its peak. At present, monitoring of water consumption is considered a key element in the artificial intelligence (AI) models used in the advanced AWM, as it forms part of the smart water management systems [7,8]. The components of these systems include leak management, flow monitoring, overuse and contamination, and devising of strategies [8]. Therefore, RS can play an important role in advanced AWM as it provides data on agricultural water requirements and available sources of water.

The use of RS to map irrigated areas and IWC contributes to advanced AWM, as irrigation is the principal consumer of freshwater resources [9,10]. Data from different RS sources provide the means to monitor IWC and water resources through mapping of crop evapotranspiration (ET) [11], which is a major component of crop water consumption [12,13]. The use of in situ instruments to measure ET for large areas is impractical, implies high investment and maintenance costs [14,15], and requires homogeneous surfaces [16]. The methods of ET estimation, on the other hand, require good spatial distribution of climatic data and the availability of detailed information on crop management. Therefore, different RS-based methods have been developed to map ET with minimum ground data [17]. These include the surface energy balance models [18–20], the reflectance-based basal crop coefficients methods [17,21], and the Penman–Monteith method [12], adapted to remote sensing input data [22].

The mapping of ET from remote sensing data has the advantages of large spatial coverage and minimum climatic and ground data [23,24], providing that calibration for ET is made to minimize uncertainties in ET estimates [24–26]. Among the RS-based models that provide ET estimates from Landsat data are the single-source surface energy balance models known as METRIC (mapping evapotranspiration with internalized calibration) [19] and SEBAL (surface energy balance algorithm for land) [20]. The level of accuracy for ET maps from SEBAL, METRIC, and other RS-based ET models depends on several factors. These include the environmental conditions of the irrigated area, crop type, irrigation management, the model itself, and the quality of data used in the model [27–37]. Variations between modeled and measured ET are usually observed in inter-seasonal and daily ET estimates [28,33], while errors in modeled ET average out for large areas and for annual time steps [38].

Remote sensing maps of irrigated crops and ET are important for AWM as they provide spatial information on annual IWC and identify periods when agricultural water demand and consumption are high. Such information is important for making decisions related to planning of agricultural water resources, particularly in countries like Jordan, where water resources are scarce and depleted. Considering renewable freshwater resources and the gross domestic product (GDP), Jordan is ranked the second country worldwide in terms of water scarcity [39]. In Jordan, irrigated agriculture consumes more than half of the available water resources [40–42]. Therefore, the application of RS-based methods to map irrigated areas and IWC is highly important for planning water resources. The importance of using RS to support AWM stems from the fact that information on IWC in Jordan is uncertain, as updated maps of irrigated areas do not exist [43]. The figures of IWC are also based on estimates and do not consider illegal abstraction and access to water resources by farmers.

In addition, the inaccurate metering of water abstraction and consumption at farm and basin levels contribute to uncertainties in reported figures of IWC [44]. The incorrect figures of IWC make it difficult for Jordan's Ministry of Water and Irrigation (MWI) to plan the present and future water supply and demand. Therefore, geospatial techniques of RS and GIS have been adopted by the MWI to update figures of IWC and groundwater abstraction.

In the context of water management in Jordan, the use of RS to monitor IWC and to predict future demand is very important. Although previous studies [45–47] showed that the water scarcity problem cannot be remedied only through improved water management, the use of RS-based methods to monitor water resources is crucial for better governance and decentralization of water management. In terms of governance, the use of RS contributes to efforts of the MWI in controlling the illegal access to water, which results in intermittency of the public water network [48], and in reducing groundwater abstraction. Both aspects contribute to the increased volume of non-revenue water, which is considered as a major shortcoming in water governance in Jordan [45]. In terms of groundwater abstraction for irrigation, the rates or volumes are higher than what the MWI data suggest [43,44,49,50]. Calculation of these volumes, therefore, is important for decentralized water management. Furthermore, it will provide the MWI with information needed for supply-based water allocation and for controlling groundwater abstraction in areas where abstraction is exceeding the safe yield.

Although the water insufficiency emphasizes factors external to the responsibility of the Jordanian government [46,47], control of non-revenue water will indirectly increase water supply. This can be achieved by possible water savings that can be reached by the use of RS to uncover illegal abstraction of groundwater [44]. The improvements in spatial, spectral, and temporal resolutions of the free data of RS can contribute to these aspects of water management in Jordan and in water-scarce countries. The challenge, however, will be the use of methods that require minimum ground data. Therefore, this study shows how RS data were used to map irrigated crops and IWC in Jordan during 2017–2019, a period that had detailed water budgets prepared by the MWI [40–42]. The study has multidimensional objectives that include accurate estimates of IWC and spatial maps of irrigated crops and hotspots where groundwater is depleted. In terms of RS methods, the study makes a novel contribution by presenting detailed methods that enable accurate mapping of irrigated crops and IWC. The novel contribution also includes the development of relationships that correlate the normalized difference vegetation index (NDVI) with the crop coefficient (Kc). These relationships are important to derive ET, which in turn can be converted to IWC using ground data. The study also utilizes present and historical RS data to provide forecasts for IWC in the future (year 2050). The work of crop mapping started in 2017 and commenced by 2020, while analysis of data extended to 2021.

2. Materials and Methods

2.1. Study Areas

The study covered all irrigated areas in Jordan, which has a total area of 89.5 thousand km^2 and altitudes ranging from –425 m at the Dead Sea up to 1750 m at Jebel Rum in the south. The country has three distinguished climatic zones (Figure 1). The first zone is Jordan Valley (JV), which is situated below the mean sea level and has a subtropical climate with warm winters and hot summers. In this zone, irrigation is managed by JV Authority (JVA) who supplies water to farmers to irrigate citrus, date palm, fruit trees, and vegetables (during winter and spring). Irrigation water sources include surface water, treated wastewater (TWW) mixed with freshwater, and groundwater. The second zone includes the Mediterranean highlands east of JV, where precipitation is in the range of 200 to 600 mm. In this zone, irrigation is practiced in spring and summer using groundwater (main source) and TWW in a few locations. The third zone is known as the "Badia" and includes arid and hyper-arid areas (desert), where rainfall decreases from 200 mm in the west and north to less than 70 mm in the east and the south.

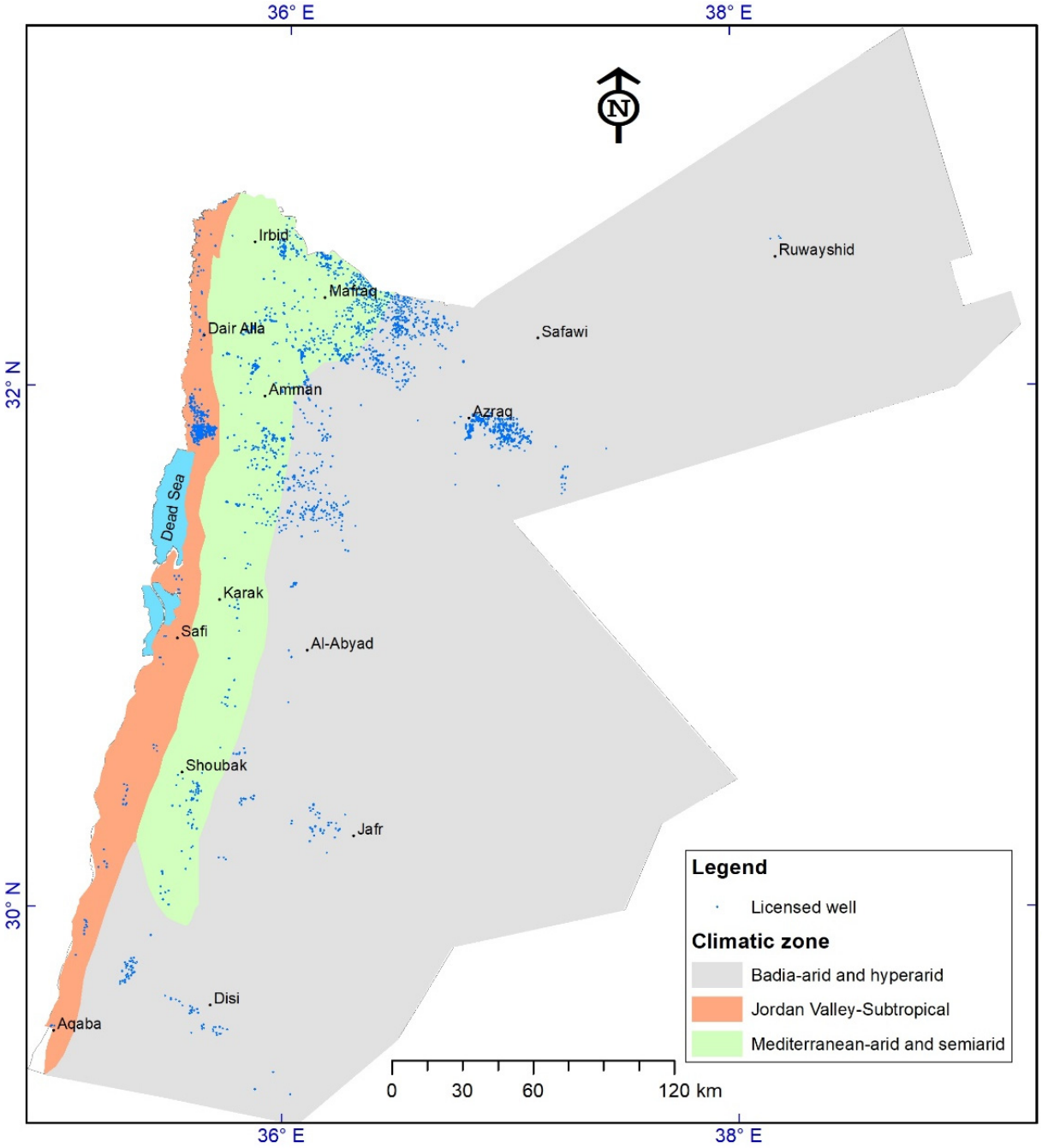

Figure 1. Locations of the study areas' groundwater irrigation wells in Jordan.

2.2. Collection and Pre-Processing of Data

Remote sensing data of Landsat 8 and Sentinel-2 images were used to map irrigated crops and IWC. The data of Landsat have a spatial resolution of 30–100 m and a temporal resolution of 16 days [51], while the data of Sentinel-2 have a resolution of 10–60 m and a temporal resolution of 5 days [52,53]. Both datasets were downloaded "https://earthexplorer.usgs.gov/" (accessed on 28 November 2022) for years 2017, 2018, and 2019 and used to map irrigated crops. Cloud-free images of Landsat 8 (Appendix A) were used in the SEBAL model to derive ET, while Landsat 7 images were only used when cloud-free images of Landsat 8 were not available. Images of Landsat were transformed into NDVI layers using the red and near-infrared (NIR) bands. These were bands 4 and 5

for Landsat 8 and bands 3 and 4 for Landsat 7. For Sentinel-2, NDVI layers were derived from bands 8 and 4 and were used to map some irrigated crops in JV, as described by Al-Bakri et al. [54]. Depending on the location of irrigated area and cloud cover, the number of Landsat NDVI layers processed for each year during 2017–2019 ranged between 18 to 21 images (Appendix A).

Hourly and daily climatic data for years 2017, 2018, and 2019 were obtained from the MWI and from the Jordan Meteorological Department (JMD). Both climatic data and Landsat images were used in SEBAL to derive maps of ET. GIS layers for farm units in JV, springs and licensed groundwater wells, wastewater treatment plants (WWTPs), and water reservoirs were obtained from MWI and JVA. These maps aided in identifying irrigated areas or locations where irrigation might be practiced. Data for irrigated farm units in JV included the code of each farm unit, crop type, areas of irrigated crops inside each farm unit, and the annual amount of water pumped to that unit. Ground surveys were also carried out to verify maps of irrigated crops and volumes of water used for irrigating some crops, particularly vegetables grown under plastic houses. The methodology used in this study is summarized in Figure 2.

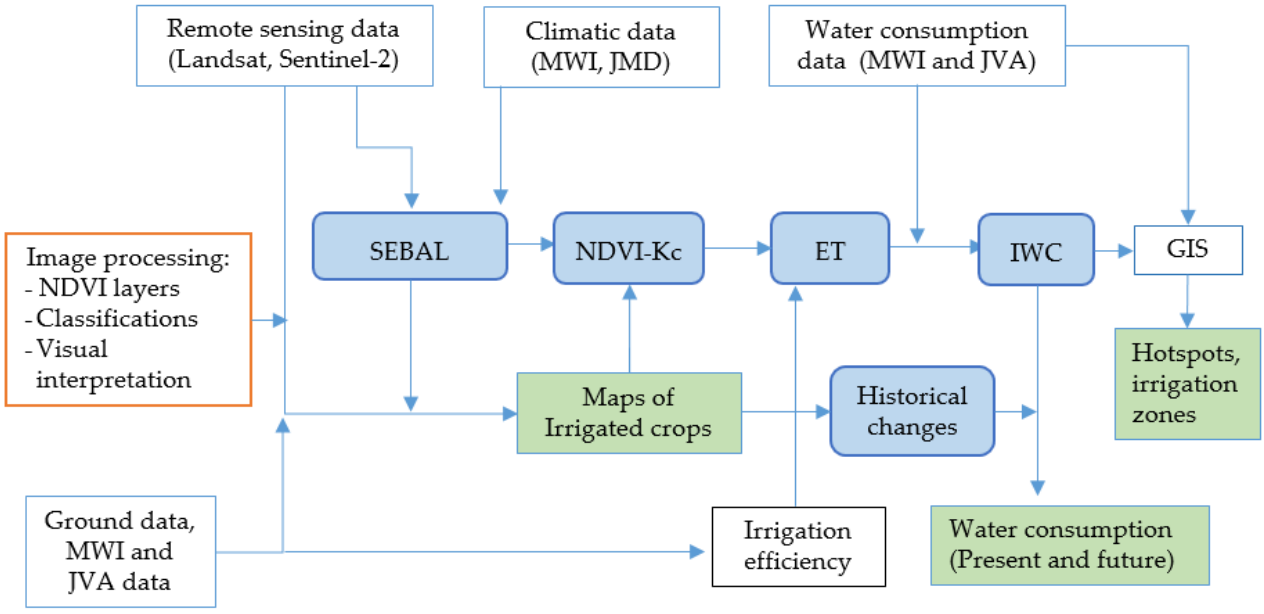

Figure 2. Flowchart of the study methodology.

2.3. Mapping of Irrigated Crops

Due to variations in climate, crop type, and cropping calendars among the irrigated areas, different methods were used to map irrigated crops and IWC. The methods were based on the use of different digital image classification techniques and visual interpretation to derive crop maps from the multi-temporal satellite images of Landsat 8 and Sentinel-2. For each year during 2017–2019, multi-temporal images of Landsat were transformed to NDVI layers that covered all growing seasons. Digital image processing techniques were applied to derive maps of irrigated crops grown in open fields. Visual interpretation of Sentinel-2 was used to map vegetable crops grown under plastic houses. Ground surveys and JVA data were used to assess and improve the accuracy of mapping.

The most commonly used techniques of digital classification for land cover and crop mapping are the parametric methods of supervised and unsupervised clustering applied to a single multispectral image [55,56]. More advanced techniques include non-parametric machine learning, which utilizes ground data and knowledge of the classifier [5]. For irrigated crops, methods that combine parametric and non-parametric algorithms of multi-

temporal RS data can improve the accuracy of mapping [5,55,57,58]. The methods used in this study included the use of unsupervised classification, decision-tree- or knowledge-based classification that utilized NDVI during the growing season, and density slicing of the annual sum or composites of maximum NDVI. Outputs from classification included irrigated and non-irrigated areas. Maps of SEBAL-ET, ground data, and GIS layers of farm units (only in JV) were used to identify the type of irrigated crop. Accuracy of classifications were assessed using class agreement for the irrigated parcel or fields rather than using the time-consuming confusion matrices applied for classified pixels [59,60]. Visual interpretation of Sentinel-2 was applied using onscreen digitizing to delineate plastic houses where vegetable crops were grown, both in JV and the highlands. Manual editing for borders of irrigated parcels was carried out, and ground observations were used to correct misclassified irrigated areas. The map of 2017 served as the base for the map of 2018, which was in turn used as the base for the map of 2019. More details on crop mapping for the different irrigated areas are included in the following subsections.

2.3.1. Mapping of Irrigated Crops in Jordan Valley

The area of JV included the north Jordan Valley (NJV), the middle-south JV (MSJV), Ghor As-Safi, and Wadi Araba. The NJV and MSJV are also known as the northern and middle Ghor areas. The main source of irrigation water for NJV and MSJV is King Abdulla Canal (KAC), which carries transboundary surface water, about 17–20 million cubic meters (MCM), from Mukheiba wells and water stored in Al-Wehdah (Unity) dam and dams on the side wadis east of JV. The irrigated areas in MSJV receive lower rainfall than NJV and extend from the southern edge of NJV to the Dead Sea. The MSJV irrigated area depends on surface water and TWW delivered to KAC from King Talal Dam and privately owned groundwater wells (Figure 1). Irrigation in Ghor As-Safi depends on surface water conveyed from dams on the side wadis, while irrigation in Wadi Araba depends on groundwater.

The NJV has most of the irrigated citrus in Jordan, in addition to fruit trees of grapes and date palm, open fields of irrigated vegetables, and a small area of banana and plastic houses. The area has a relatively high rainfall that exceeds 500 mm in its northern parts and drops down to 300 mm in its southern parts. Irrigation of citrus is usually practiced during March-November. Mapping of irrigated areas in NJV included the use of unsupervised classification with the iterative self-organizing data analysis technique (ISODATA) [56] applied on the multi-temporal layers of NDVI, derived from the Operational Land Imager (OLI) of Landsat 8. The output from ISODATA (Figure 3) showed 15 distinct spectral classes that represented irrigated areas and land cover types. Irrigated fields of citrus and trees were well represented by classes 14 and 15 and were in agreement with data of farm units provided by JVA. Three images of Sentinel-2 were used to improve mapping accuracy. The first image, acquired in March, was used to derive the layer of NDVI that represented irrigated vegetables, citrus, and fruit trees. The second image, acquired in August, was used to derive the NDVI layer that represented irrigated citrus and date palm, when vegetables were not grown. The third image, acquired in November, was used to derive the NDVI layer and represented irrigated citrus, date palm, and vegetables. Ground surveys and JVA data were used to verify mapping results and to separate parcels of irrigated cereals and fodders from other crops.

The same approach of unsupervised classification was used to map irrigated crops in MSJV and Ghor As-Safi. In these areas, results of digital classification showed 12 distinct spectral classes of irrigated crops and land cover. Classes that represented irrigated crops (Figures 4 and 5) were identified using JVA and ground data. The overall accuracy of mapping was 74% in MSJV and 79% in Ghor As-Safi. Different GIS functions of clipping and intersection were applied to remove non-irrigated parcels and to finalize the maps. Furthermore, misclassified irrigated farm units were corrected using JVA data and Sentinel-2 layers of NDVI, following the same procedure used in NJV.

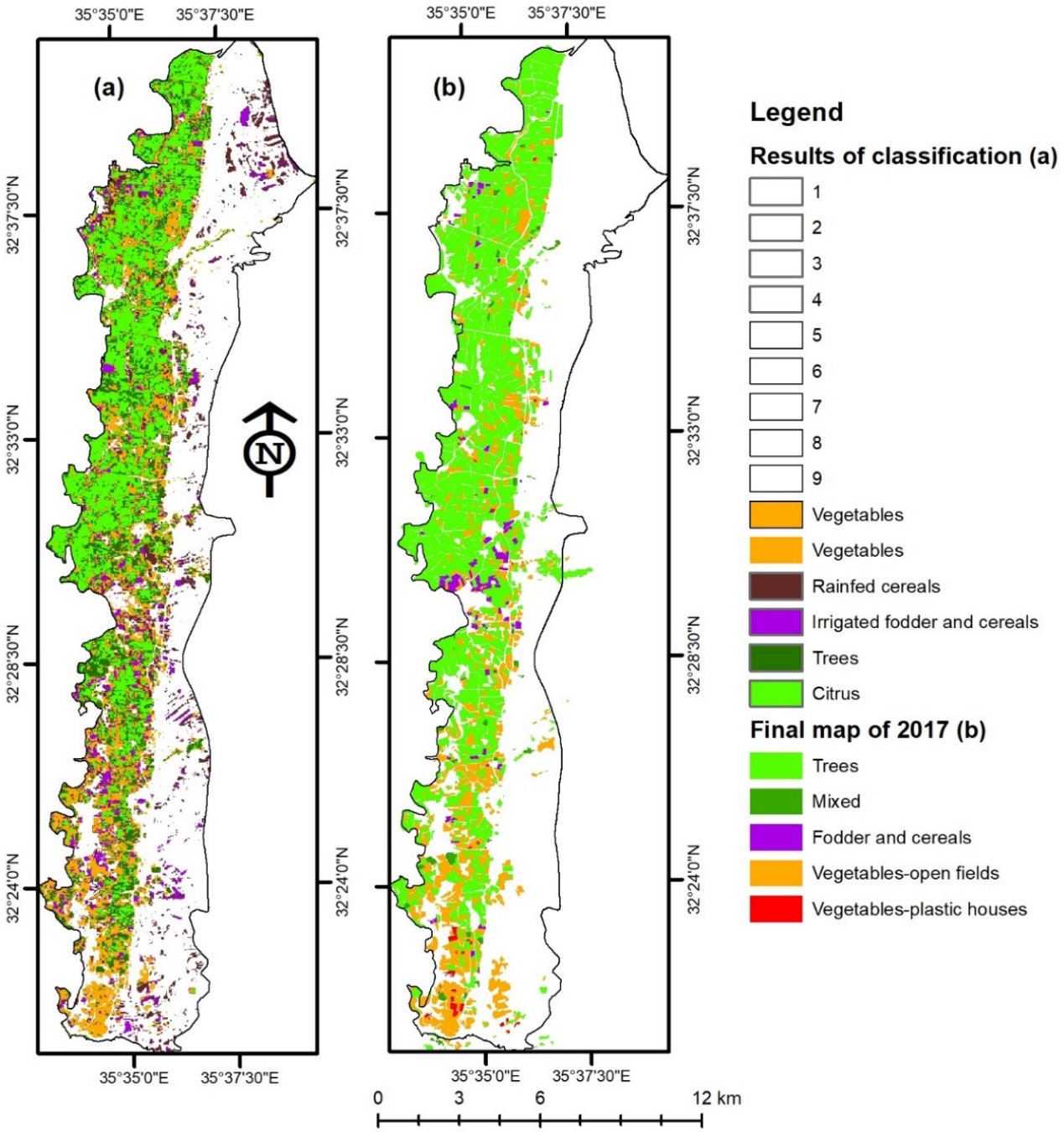

Figure 3. Results of unsupervised classification of the multi-temporal NDVI layers (**a**) and the final map of irrigated crops (**b**) for NJV in 2017.

Irrigated areas in Wadi Araba included farms of vegetable crops of tomatoes and watermelon and two farms of date palm. Two images of Sentinel-2, acquired in the periods of peak growth in April and November, were used to map irrigated farms in this area. Both images were transformed to NDVI layers that represented vegetation in this dry area. Manual editing was used in GIS to remove parcels that represented natural vegetation in three wadis to the south of Graigrah and Feinan villages. For all irrigated areas in the JV area, a majority filter with a 3-by-3 kernel was applied on the outputs from digital classification. This noise removal filter was applied to remove isolated pixels (islands) and to have homogenous parcels of irrigated areas.

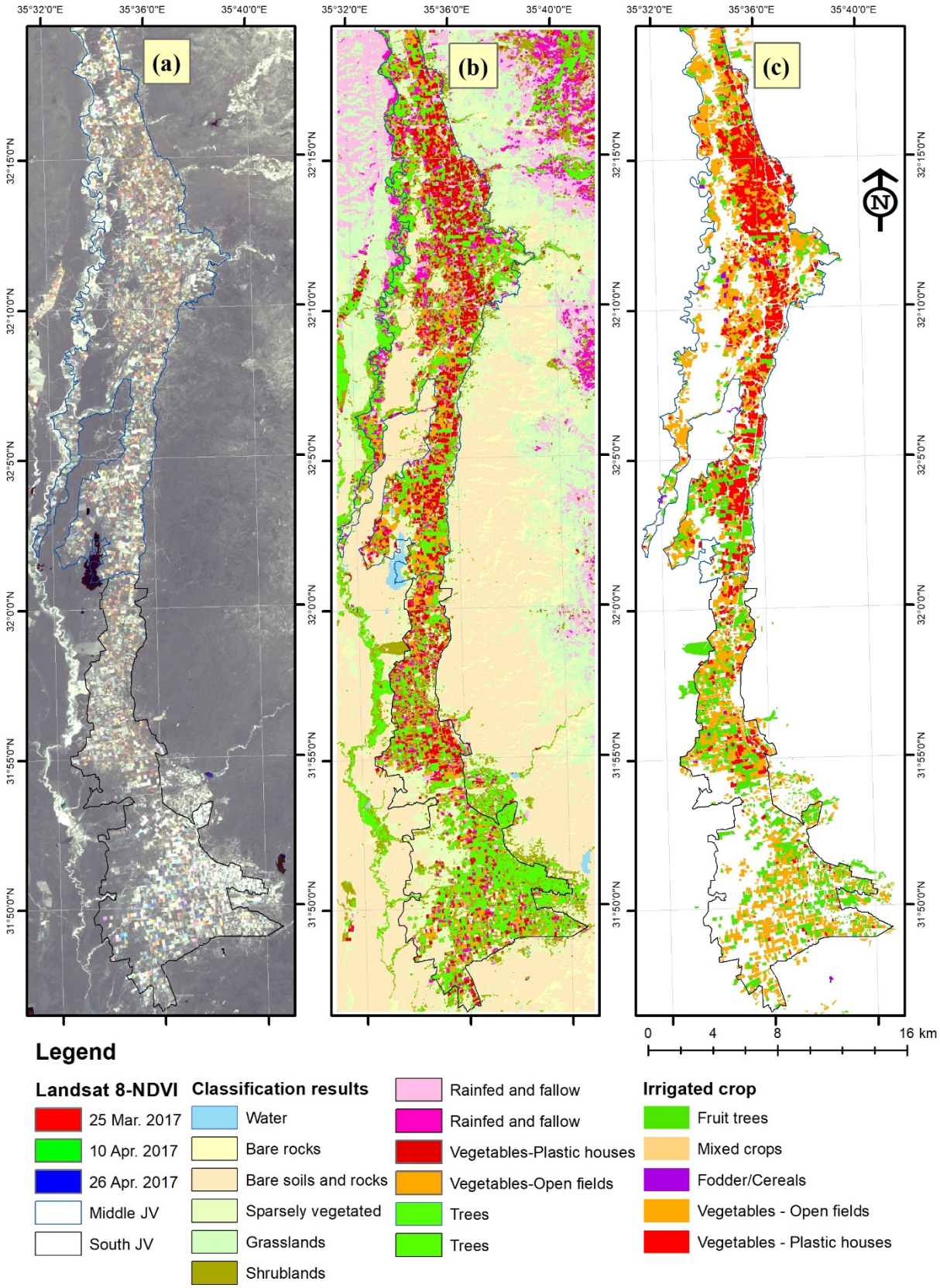

Figure 4. Mapping of irrigated crops in MSJV. (**a**) Multi-temporal NDVI layers covering the whole year; (**b**) Results of the unsupervised classification of the NDVI images; (**c**) Final map of irrigated crops after editing, merging of ground data, and applying different GIS overlay functions.

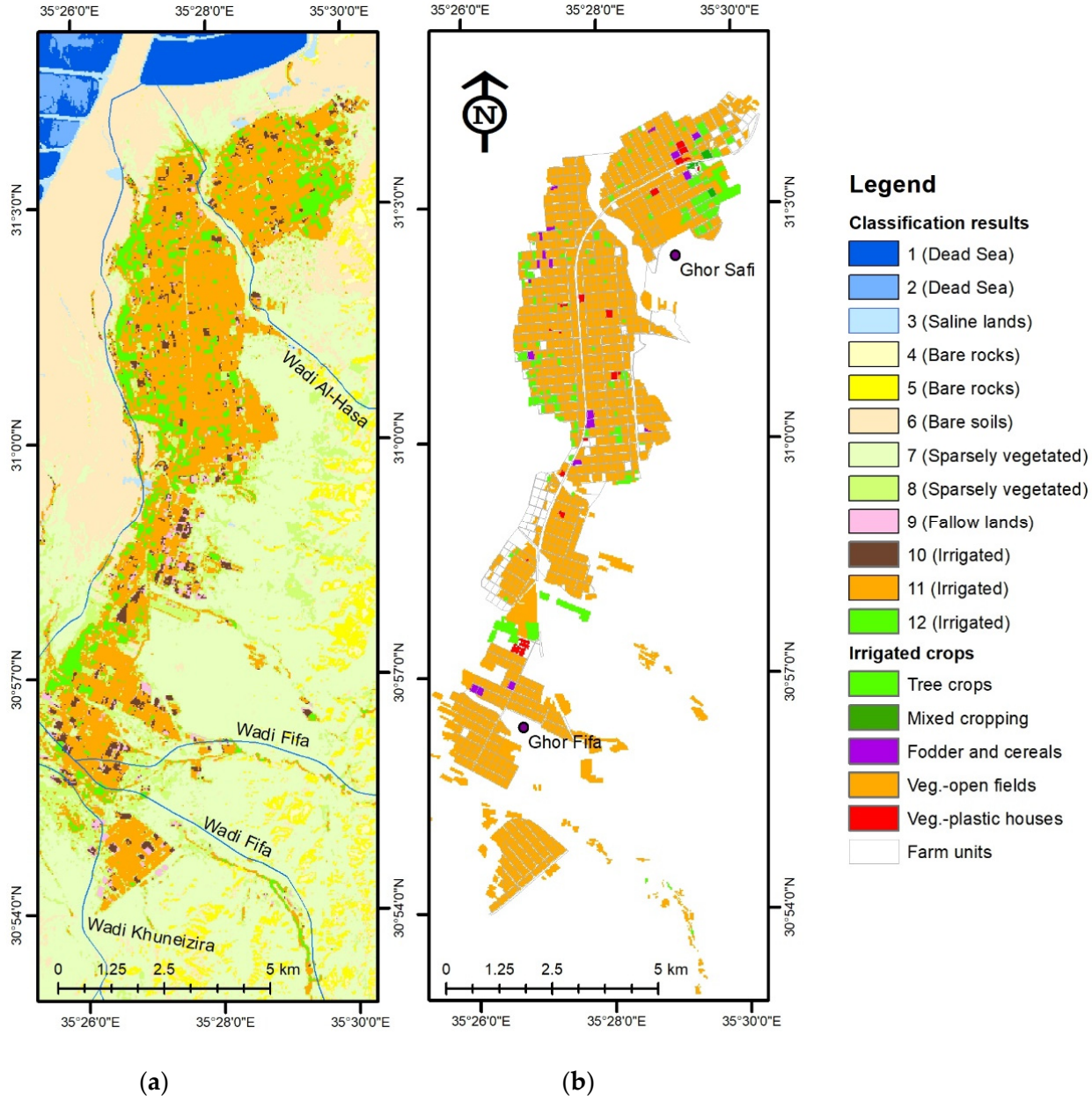

Figure 5. Mapping of irrigated crops in Ghor As-Safi. (**a**) Results of the unsupervised classification of the multi-temporal NDVI images; (**b**) Final map of irrigated crops after editing, merging of ground data, and applying different GIS overlay functions.

2.3.2. Mapping of Irrigated Crops in the Mediterranean Highlands

Irrigated areas in the Mediterranean highlands depend mainly on groundwater and to a lesser extent on springs, TWW, and surface water. Irrigated crops of vegetables are cultivated in two seasons: February to June and July to October. Forage crops of alfalfa are also cultivated near WWTP, while fruit trees are irrigated during May-September. Generally, no irrigation takes place during December-February, while little supplemental irrigation may take place during March. Mapping of irrigated areas in the highlands was based on the unsupervised classification of the Landsat NDVI multi-temporal layers that covered the period of March-October. Initial results of classification (Figure 6) showed 10 spectral classes that were identified and separated based on ground data and layers of SEBAL-ET. The use of SEBAL to derive the ET map for the spring and summer months, i.e., outside the rainy season, enabled the separation of irrigated areas from the rainfed areas, as irrigated areas were characterized by relatively high ET compared to rainfed areas. For most of the

irrigated areas in the Mediterranean highlands, the annual ET was more than 700 mm for fodder, 400–700 mm for fruit trees, and 200–400 mm for vegetables.

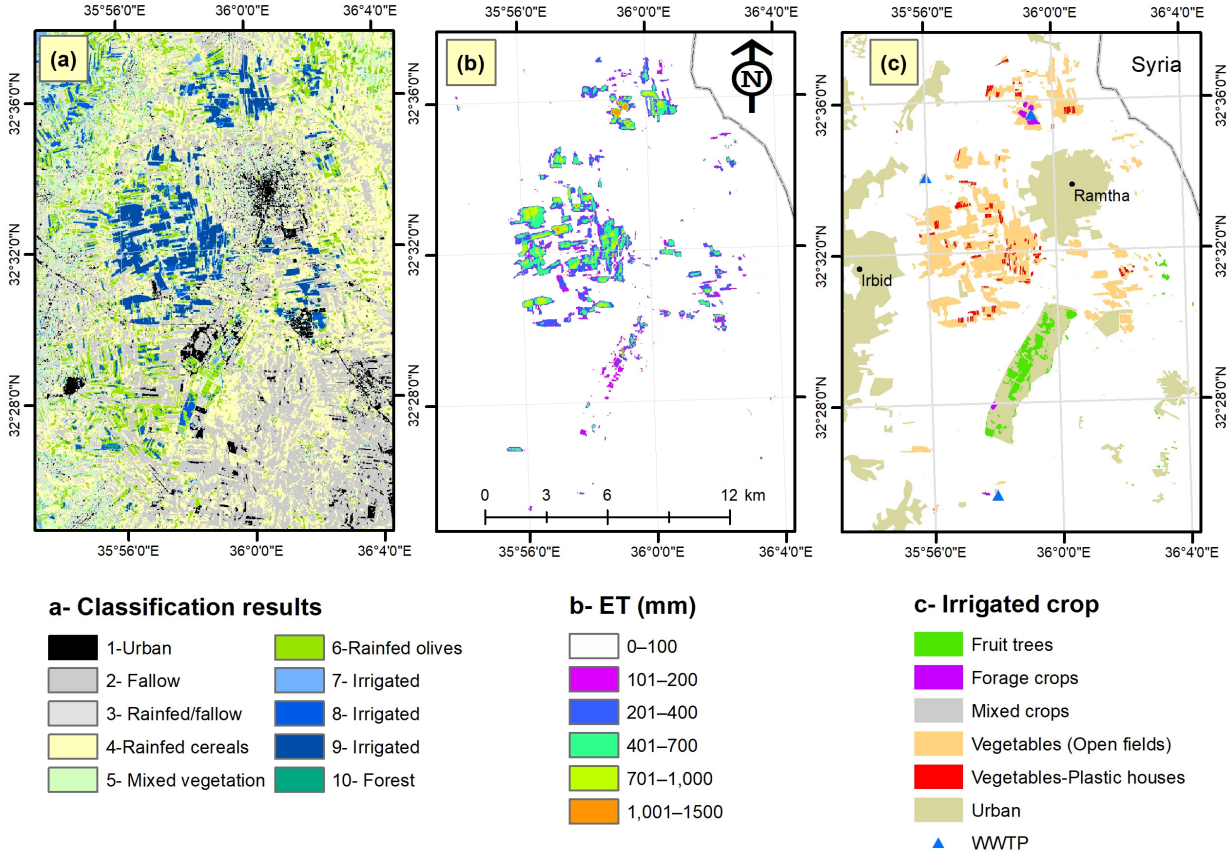

Figure 6. An example of mapping irrigated crops in the Mediterranean highlands for the area of Irbid-Ramtha. (**a**) Results of the unsupervised classification of the multi-temporal NDVI images for the period March-October; (**b**) SEBAL-ET map for March-October; (**c**) Map of irrigated crops after merging digital classification with SEBAL-ET.

2.3.3. Mapping Irrigated Crops in the Badia

Irrigation in Badia is mainly practiced in the arid area of Mafraq (Figure 7) and in the hyper-arid (desert) areas of Azraq, Hallabat, south and southeast of Queen Alia International Airport (QAIA), Jafr, and Quwayrah-Disi (Figure 8). An obvious expansion in irrigation took place in the Badia, especially in Mafraq, where fruit trees (peaches, apricots, olives, and grapes) and vegetables are grown. In terms of crop mapping, previous work in this area [43] showed that the use of unsupervised classification did not enable the full detection of all irrigated areas. Therefore, a decision tree (knowledge-based) classification was used for mapping irrigated crops in this area. Layers of seasonal sum and maximum NDVI were used to identify the type of crop. Results showed that the maximum NDVI value was the best identifier for irrigated crops. These were characterized by an NDVI-maximum value larger than 0.30 for the period May-November (Figure 7). Decision on the type of crop was based on conditional statements that included the range of NDVI value during the growing seasons [43]. Mapping of irrigated crops in the desert areas of the Badia was based on the unsupervised classification of multi-temporal NDVI layers, density slicing of the annual sum of NDVI, maps of SEBAL-ET, and ground surveys. Generally, irrigated areas in these desert areas were accurately detected using the aforementioned methods. Errors in mapping were only observed in areas with dense vegetation in the waterways. These were manually removed in GIS.

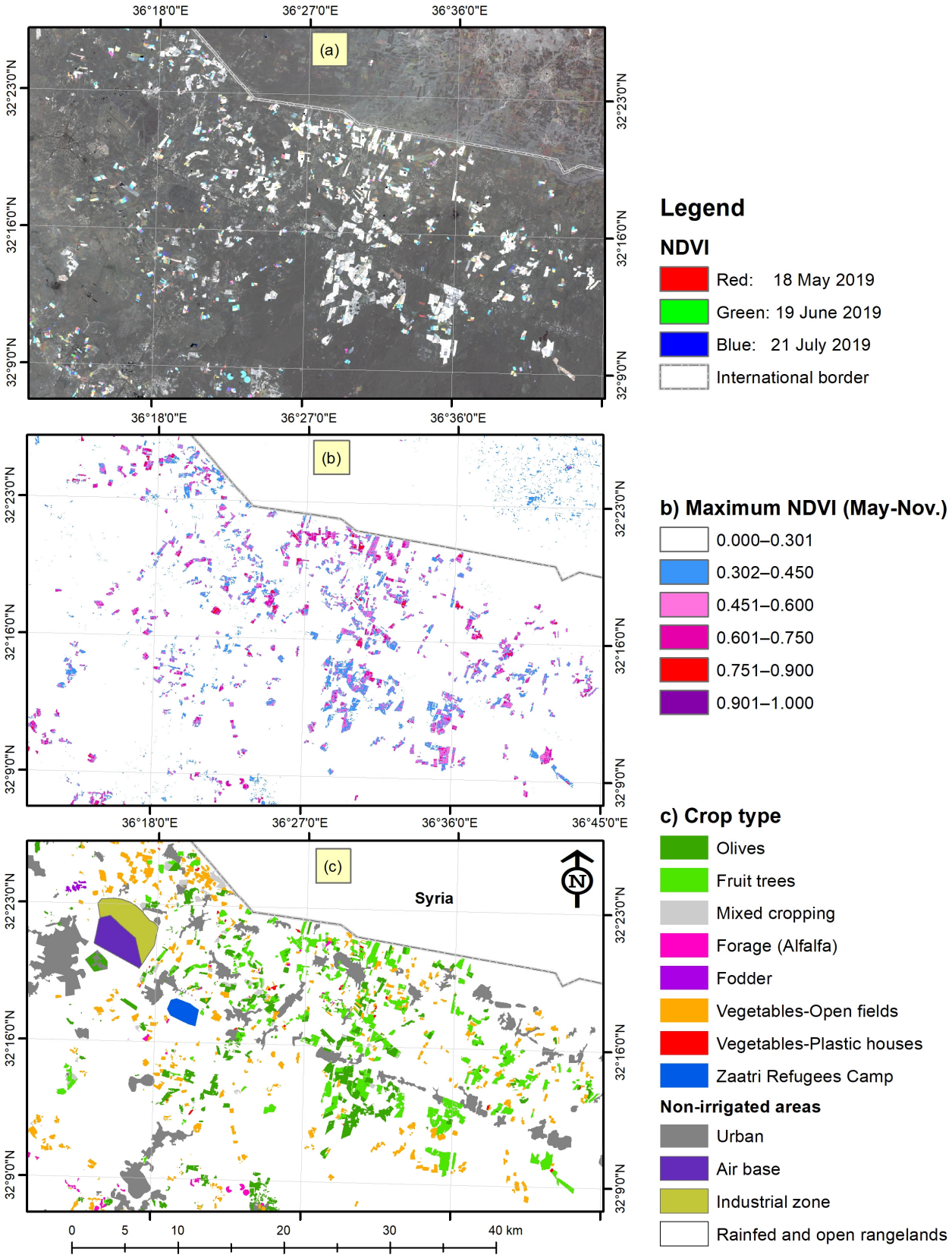

Figure 7. Mapping of irrigated crops in Mafraq. (**a**) Example of the multi-temporal NDVI layers covering the whole year; (**b**) Detection of irrigated parcels through density slicing of maximum NDVI value during May-November; (**c**) Final map of irrigated crops.

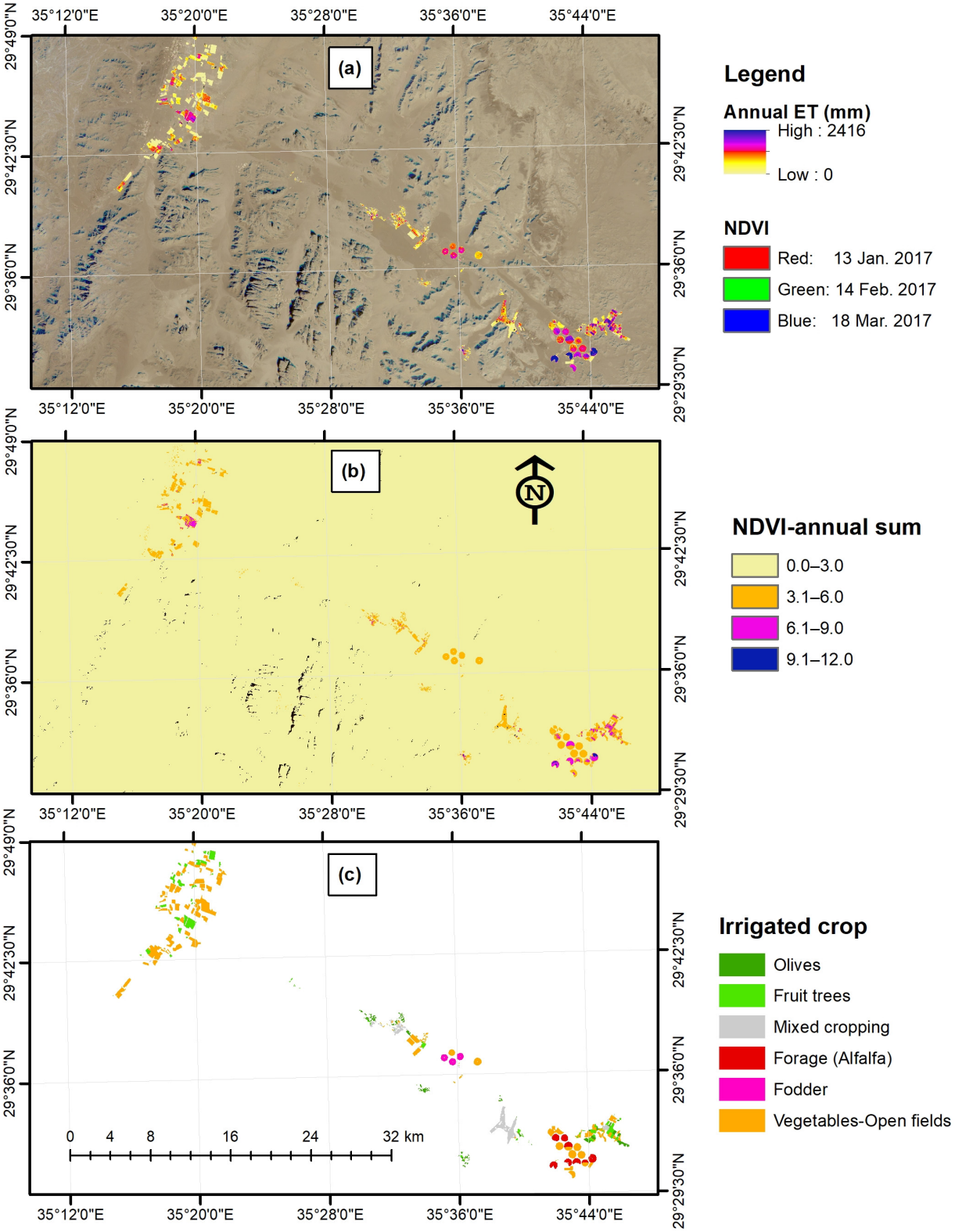

Figure 8. Mapping of irrigated crops in the desert of Badia in the Quwayrah-Disi area. (**a**) SEBAL-ET map displayed over the multi-temporal NDVI layers of 2017; (**b**) Classification of crops based on the annual sum of NDVI; (**c**) Final map of irrigated crops merging maps of ET and classified annual NDVI.

2.3.4. Mapping Historical Changes in Irrigated Areas

Historical changes in irrigated areas were mapped and analyzed to identify possible expansion and recession in irrigated areas in the future. This was carried out to calculate future agricultural water demand and to keep future changes in the context of water management. The challenge for mapping these areas was the limited historical multispectral data of satellite imagery and the lack of archived multi-temporal images. The RS data that covered the whole country included Landsat 5 and 7 for years 1987 and 2002, respectively. The approach of mapping was based on transforming images of 1987 (acquired in April and May) and 2002 (acquired in March) to NDVI layers using bands 3 (red) and 4 (NIR). The NDVI layers were converted to shapefiles that represented vegetated and rainfed areas. Decisions on irrigated areas were based on visual interpretation, data of water source, agricultural census from the Department of Statistics (DOS) [61], and the data of JVA, in addition to data and findings from previous studies [62–64]. The rate of change in irrigated area in the future was based on the rate of change during the period 2002–2017, following the enforcement of water law in Jordan. Modifications to future irrigated areas inside the different zones were carried out, depending on the availability of water resources in the future.

2.4. Mapping of ET and IWC

Mapping of ET was carried out using the SEBAL model, which incorporated Landsat and hourly and daily climatic data. SEBAL computes the components of energy balance from the incoming solar radiation for each pixel. ET is derived in terms of instantaneous latent heat flux or λET (W m^{-2}), and it is computed as the residual of the surface energy balance equation at the moment of satellite overpass on a pixel-by-pixel basis as follows [20]:

$$\lambda ET = (Rn - G - H) \quad (1)$$

where Rn is net radiation (W m^{-2}), G is the soil heat flux (W m^{-2}), and H is the sensible heat flux (W m^{-2}).

The steps for deriving the components in equation 1 are described by Bastiaanssen et al. [20]. In summary, the main output from SEBAL is the evaporative fraction (ETrF), which is calculated as follows:

$$ETrF = ET_{inst}/ETr \quad (2)$$

where ET_{inst} is the instantaneous ET (mmh^{-1}) and ETr is the standardized 0.5 m-tall alfalfa reference ET (mmh^{-1}) at the time of the image [19,20]. ETrF is similar to the well-known Kc and corresponds to the actual rather than the theoretical Kc.

The total ET for each pixel and for the period represented by each Landsat scene (16 days) was calculated by summing ETr for this period and multiplying it with ETrF [19,20]. The annual ET maps were derived by summing all layers of ET generated by SEBAL for every 16 days. Since hourly climatic data, needed to run SEBAL, were not available for all irrigated areas, the model was run for areas where hourly data were available. Outputs were used to develop relationships between NDVI and Kc or ETrF. The NDVI-Kc relationships for the different irrigated crops were then used to derive ET maps for areas that lacked hourly climatic data in the year 2017 and for all irrigated areas for the years 2018 and 2019. The relationship of NDVI-Kc for different crops was developed using data for farms with well-watered crops. The farms included the crops of alfalfa in Azraq and Jafr, fruit trees and vegetables in Mafraq and JV, citrus in NJV, and mixed crops in Azraq.

Maps of SEBAL-ET were converted to maps of IWC using ground data of water consumption at the farm level (Appendix B). The advantage of this approach over the conventional approach that converts the net irrigation water requirement (NIWR) to gross irrigation water requirement (GIWR) is that it does not require intensive ground measurements of soil water balance and farm irrigation efficiency. Instead, it converts ET directly to IWC based on actual consumption or abstraction of water used by farmers. The data for converting ET to IWC were obtained from JVA, governmental irrigation projects, and

private farms that purchased groundwater from private or governmental groundwater wells. Furthermore, it included locations where TWW is used to irrigate fodder crops. Appendix B includes examples of these locations and information on crops and the ET-IWC conversion factors in the different irrigated zones in Jordan. Data on IWC for vegetables grown under plastic houses in the highlands were obtained from farmers in Irbid-Ramtha and in the area south of Amman-QAIA.

Results for irrigated areas and IWC were summarized for the period 2017–2019, using descriptive statistics. Two performance metrics (statistical parameters) were used to assess the degree of correlations between the ET modeled from NDVI-Kc relationships with SEBAL-ET. These were the root mean square error (RMSE) and the Nash–Sutcliffe model efficiency coefficient (NSE), as shown in the following equations [65,66]:

$$\text{RMSE} = \left[n^{-1} \sum_{i=1}^{n} \left(Y_i^{sim} - Y_i^{obs} \right) \right]^{0.5} \quad (3)$$

$$\text{NSE} = 1 - \left[\frac{\sum_{i=1}^{n} \left(Y_i^{sim} - Y_i^{obs} \right)^2}{\sum_{i=1}^{n} \left(Y_i^{obs} - Y^{mean} \right)^2} \right] \quad (4)$$

where Y_i^{sim} is the ith simulated value (ET from the NDVI-Kc relationship), Y_i^{obs} is the ith observed value (SEBAL-ET), Y^{mean} is the mean of observed data (SEBAL-ET), and n is the number of observations. NSE ranges between $-\infty$ and 1.0 (1 inclusive), with NSE = 1 being the optimal value. Values between 0.0 and 1.0 are generally viewed as acceptable levels of performance, whereas values <0.0 indicates unacceptable performance [66].

2.5. Application of Spatial Analysis

In order to identify hotspots where shifts in ET and water consumption were evident, GIS was used to convert maps of ET and groundwater abstraction to density maps that show levels of ET and abstraction in mm/km^2. Spatial interpolation was used to convert maps of groundwater wells (Figure 1) to maps of groundwater abstraction using the attribute of annual volumes pumped by farmers. The inverse distance weighted (IDW) method, an exact interpolator [67], was used with a squared exponent of distance to give more weight to the location of the groundwater well. Density analysis [68] was applied on maps of annual ET to derive amounts of consumptive use per unit area. The point kernel method of density mapping was carried out using a neighborhood circular distance of 5 km. The distance was based on field observations and previous work [43], which showed that many farmers in the highlands were selling and/or conveying water for long distances that reached 5 km. In the context of AWM, the aim of the density analysis was to show areas where ET was concentrated so that zones with high water consumption were identified and delineated for future planning of water supply and demand. In addition, overlaying the ET density map with the groundwater abstraction map showed areas where shifts between both maps existed. These locations were identified as hotspots where farmers might have illegal access to water sources. Maps and coordinates of hotspots were provided to the MWI so that campaigns were oriented towards these locations to uncover and to control illegal access to water. An example of one of the hotspots in Azraq is presented in this study. Volumes of water savings from the non-revenue water are included in reports provided to MWI (e.g., [42]), while results in this study present the total water savings at the levels of irrigated zones and the country.

3. Results

3.1. Accuracy of Mapping Irrigated Crops from Remote Sensing Data

Table 1 summarizes the accuracy of the methods applied to map irrigated crops in Jordan. In general, mapping accuracy was relatively high, particularly in the desert areas of the Badia, where little mixing occurred among the classes of irrigated crops. In NJV,

spectral mixing between vegetables and cereal crops resulted in lowering the accuracy of mapping for vegetables to 78%, while citrus was mapped with an overall accuracy of 92%. Mapping accuracies in MSJV and Ghor As-Safi were 85% and 89%, respectively. Accuracy of maps for irrigated crops in Wadi Araba reached 92%. In Badia, mapping accuracy ranged between 81% in Mafraq to 94% in Quwayrah-Disi.

Table 1. Summary of digital classification methods and their accuracy.

Method	Areas Applied in for Mapping	Class Accuracy Range (%)	Data Used to Improve Accuracy and Finalize Maps
Unsupervised classification of NDVI layers	NJV, MSJV, and Ghor As-Safi	78–89	GIS layers of JVA, Sentinel-2 NDVI layers
	Highlands	82–87	SEBAL-ET, GIS layers of water resources
Density slicing of NDVI images of Sentinel-2	Wadi Araba	89–92	GIS layers of groundwater wells
Density slicing of annual sum of OLI-NDVI layers and decision tree based on NDVI profiles	Badia	81–94	SEBAL-ET, GIS layers of groundwater wells

3.2. Irrigated Areas in Jordan

Results showed that the total irrigated areas in Jordan were 96 thousand ha in 2017, 95 thousand ha in 2018, and 98 thousand ha in 2019 (Table 2). On average, irrigated areas in the highlands formed 65% of the total irrigated area in Jordan. Analysis of the maps of irrigated crops (Figure 9) showed that the total area of lands where irrigation was practiced during 2017–2019 was 133 thousand ha. Irrigated areas slightly increased in the year 2019 when compared with 2018 and 2017. Analysis of irrigation maps showed that vegetable crops and trees constituted 55% and 41% of the total irrigated area, respectively (Table 2). Variations in cropping patterns were observed among the different irrigated zones in both JV and highlands. In highlands, most of the irrigated areas were concentrated in the area of Mafraq and to the south of Amman.

Table 2. Summary of area (ha) for irrigated crops in Jordan during 2017–2019.

Crop	Highlands (HL)	Jordan Valley (JV) [1]		Min.[2]	Max.	Mean	S.E.	C.L.	% of the Crop
Vegetables—open fields	Open fields cultivated with tomato, watermelon, melon, pepper, potato, and other vegetables.	Farm units cultivated with tomato, eggplant, pepper, potato, onion, okra (NJV), and other vegetables.	HL	24,837	27,332	26,312	755	3250	27.3
			JV	15,159	18,760	17,302	1095	4710	17.9
			Total	42,491	45,528	43,615	962	4137	45.2
Vegetables—plastic houses	Tomato, cucumber, and other crops grown under plastic houses in spring and summer.	Tomato, cucumber, strawberry, beans, and others. Includes nurseries and multi-spans.	HL	1642	2548	2101	262	1126	2.2
			JV	3958	4083	4027	37	158	4.2
			Total	5725	6589	6128	251	1080	6.4
Trees	Olives, deciduous trees of stone fruits, peaches, apricot, date palm, apples, and grapevines.	Citrus, date palm and grapevines, fruit trees, olives, and banana.	HL	24,615	25,102	24,893	145	623	25.8
			JV	11,336	12,103	11,597	253	1089	12.0
			Total	36,314	36,718	36,490	119	514	37.8
Mixed crops	Farms cultivated fruit trees and vegetables, olives and alfalfa, and nurseries.	Parts of farm units cultivated with fruit trees, vegetables, and cereals. It also includes nurseries.	HL	4220	5397	4955	370	1592	5.1
			JV	367	529	438	48	206	0.5
			Total	4637	5777	5393	378	1626	5.6
Fodders and cereals	Open fields cultivated with fodder, forage, and cereal crops.	Farm units cultivated with wheat and barley under supplementary irrigation or alfalfa with full irrigation.	HL	3949	4596	4344	200	860	4.4
			JV	290	580	438	84	360	0.5
			Total	4239	5066	4782	272	1169	4.9

Table 2. *Cont.*

Crop	Highlands (HL)	Jordan Valley (JV) [1]		Min.[2]	Max.	Mean	S.E.	C.L.	% of the Crop
			HL	61,573	63,256	62,605	522	2245	64.7
		Totals for Jordan	JV	32,039	35,149	33,802	922	3965	35.3
			Total	95,295	98,135	96,407	876	3768	100

[1] Figures for Jordan Valley include Ghor As-Safi and Wadi Araba. [2] Min. = minimum, Max. = maximum, S.E. = standard error, C.L. = confidence level (95%).

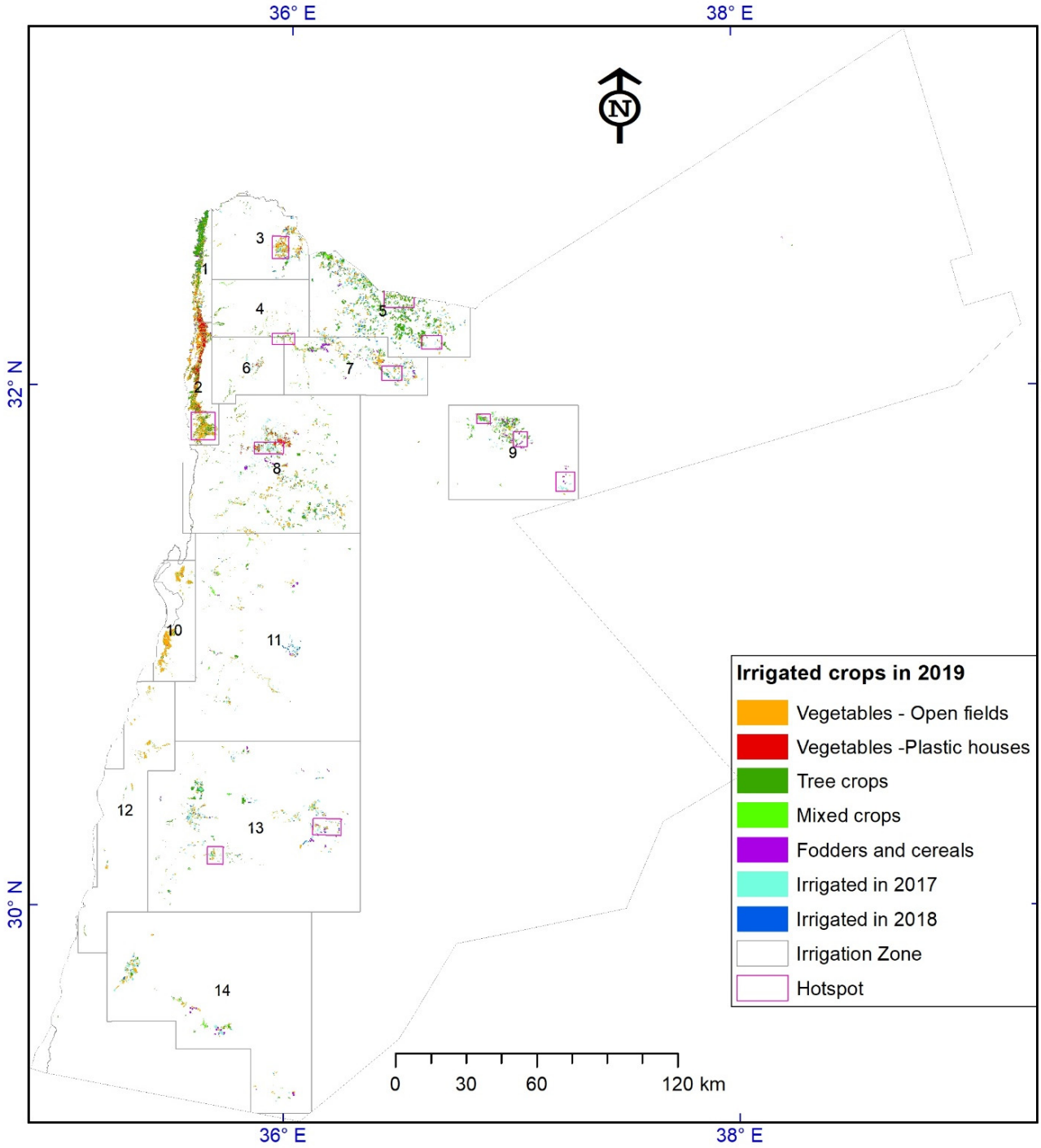

Figure 9. Map of irrigated crops in Jordan during 2017–2019 with the main irrigated zones and hotspots that have illegal access to water.

3.3. Remote Sensing of ET and IWC in Jordan

Variations were observed in the spatial distribution of remotely sensed ET in the different climatic zones in Jordan. The map of ET density for the year 2017 (Figure 10), therefore, was utilized to delineate the main irrigated zones in Jordan. Analysis of ET maps for the irrigated zones showed that JV and Mafraq zones were the main consumers of irrigation water in Jordan. The map of ET showed other important irrigated zones where hotspots with high ET existed. These were in Azraq, Zarqa, Amman-Madaba, Irbid-Ramtha, and Quwayrah-Disi. Similar spatial distributions of ET were also observed for ET maps of 2018 and 2019. Analysis of ET maps showed high levels of ET in desert areas and in JV. The average annual ET in Azraq in the year 2017, for example, was 935 mm, and the estimated annual IWC was 1438. The maximum annual ET for alfalfa farms in this area was more than 2400 mm. On the other hand, the average annual ET for the irrigated Mediterranean highlands was less than 500 mm. The annual ET for irrigated potatoes in the Irbid-Ramtha zone was less than 300 mm, while the annual ET for alfalfa in this zone was around 1500 mm. In JV, the annual ET was in the range of 750 mm for two seasons of vegetables and up to 1000 mm for the crops of date palm and citrus.

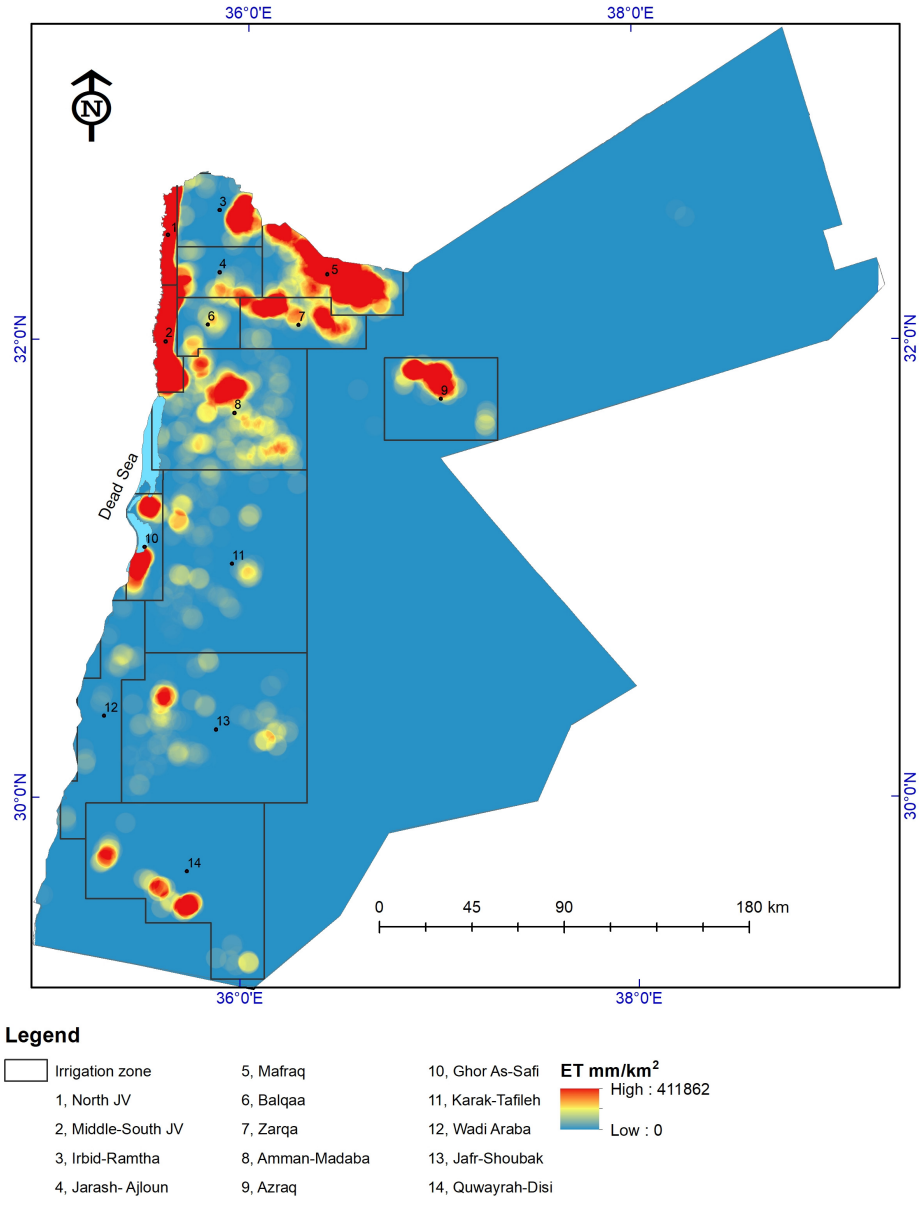

Figure 10. Map of ET density (mm/km^2) for irrigated areas in 2017 and irrigation zones in Jordan.

In terms of NDVI-Kc correlations, the study showed significant ($p < 0.05$) linear relationships between NDVI and Kc for the different irrigated crops in Jordan (Table 3). An example on the relationship between NDVI and ETrF is shown in Figure 11. The relationship between ET derived from NDVI-Kc with ET derived from SEBAL was also significant ($p < 0.05$). The value of RMSE for this relationship was relatively low (42.7), and the value of NSE was 0.89, which indicated a high performance of the NDVI-Kc model as a predictor for ET.

Table 3. Summary of the relationships between Landsat OLI-NDVI and Kc for the irrigated crops in Jordan.

Regression Parameter	Vegetables	Tree Crops	Mixed Crops	Alfalfa
Observations	47	36	34	48
Intercept (a)	−0.123	−0.080	−0.216	−0.158
Slope (b)	1.034	1.048	1.636	1.216
R^2 (Coefficient of determination)	0.887	0.912	0.928	0.918
Standard Error	0.047	0.059	0.039	0.0629

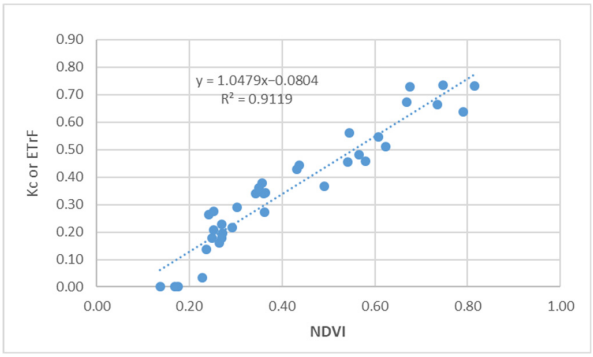

(**a**)

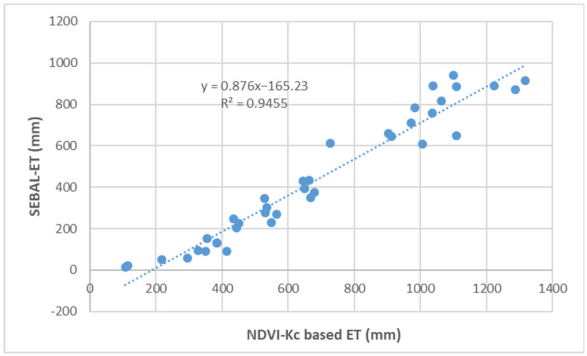

(**b**)

Figure 11. An example of the relationships used to derive ET. (**a**) NDVI-Kc relationship for vegetable crops; (**b**) NDVI-Kc-based ET vs. SEBAL-ET.

Results showed that IWC varied during the year and among the different irrigated zones (Figure 12). For example, the peak water consumption in NJV was in June, while in the Irbid-Ramtha irrigated zone, most of the water consumption took place during March-April, when irrigated potatoes reached their peak growth. In the Mafraq irrigated zone, the highest water consumption occurred during May, when vegetables were at the end of midseason. High levels of IWC in Mafraq extended during May-August, reflecting the high IWC for the cropping pattern which included both fruit trees and vegetables. Table 5 includes a detailed analysis for cropping patterns in the different irrigated zones, with a summary for irrigated areas and IWC during 2017–2019. At the level of Jordan, the

average IWC was in the range of 716–722 mm, while the total IWC for all irrigated zones reached 702 MCM in 2019. This figure represented 56% of the total water consumption in the country.

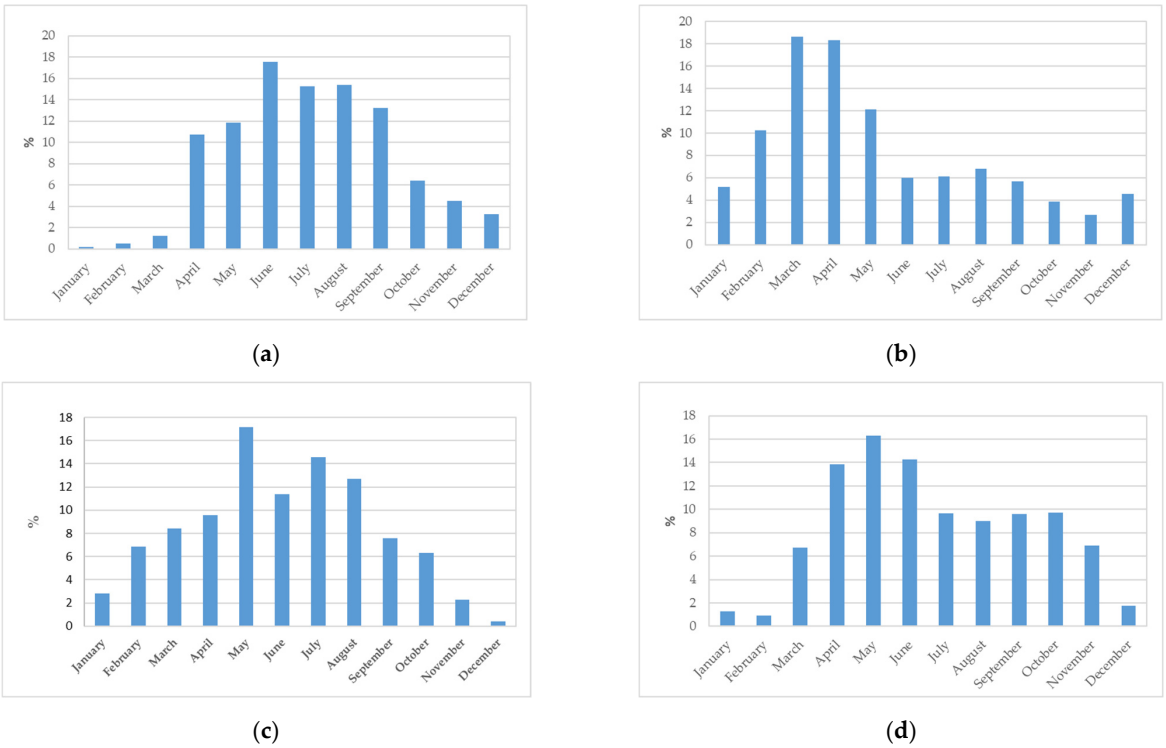

Figure 12. Distribution of IWC in some of the irrigated zones in Jordan. An example from year 2017 for (**a**) NJV; (**b**) Irbid-Ramtha; (**c**) Mafraq; (**d**) Quwayrah-Disi.

3.4. Remote Sensing and Groundwater Monitoring

Analysis of ET and IWC results in relation to recorded groundwater abstraction [40–42] and available surface water [69] showed that IWC estimated from RS methods was higher than the records of groundwater abstraction reported by the MWI. Detailed calculations of IWC and recorded groundwater volumes used in irrigation during 2019 is shown in Table 4. Results showed that IWC for all irrigated zones in Jordan was higher than the volumes reported by MWI (Table 4). The average IWC from groundwater resources exceeded the safe yield of the renewable groundwater (275 MCM). For the year 2019, RS estimates of IWC were higher than the recorded abstraction by 140 MCM, indicating high levels of water abstraction and non-revenue water, particularly in the highlands. Both remote sensing and MWI records were close to each other for the irrigated zone of Quwayrah-Disi, where groundwater wells were supervised by the MWI.

Spatial analysis of ET and groundwater abstraction maps showed 12 hotspots within the different irrigated zones in Jordan (Figure 9). In all of these hotspots, IWC was higher than the recorded abstraction of groundwater. Therefore, results of the spatial analysis for the ET and groundwater abstraction maps of 2017 and 2018 were utilized by the MWI to guide its campaigns against unlicensed groundwater wells and/or illegal access to the water network and surface water. An example for a hotspot (Hazeem) inside Azraq irrigated zone is shown in Figure 13. In this hotspot, the IWC in 2017 was 6.5 MCM, while the recorded abstraction was only 1.7 MCM. As a result of the MWI campaign, the IWC in 2018 decreased to 1.8 MCM. Similar analysis for the hotspots in the irrigation zones of Azraq showed that possible savings could reach 11 MCM if MWI would apply RS-based groundwater monitoring [44]. Similar findings with different levels of water savings were also observed for other hotspots. The total volumes of non-recorded groundwater abstraction in these areas during 2019 reached 127 MCM. Considering both IWC and

groundwater use by other sectors [40–42], the levels of groundwater abstraction were summarized for all groundwater basins in the country, as shown in Figure 14. Obviously, groundwater is over-abstracted in all basins, except Sirhan and Hamad basins, where groundwater yield is marginal.

Table 4. Irrigated area, IWC, estimated (EGW), and recorded (RGW) groundwater abstraction for the different irrigated zones during 2019.

Zone	Area (ha)	IWC (MCM)	Irrigation Water Sources (MCM)			
			Surface *	TWW	EGW	RGW
North JV	11,120	96.2	76.5	–	19.7	18.2 **
Middle-South JV	17,265	164.5	126.6	–	37.9	15.4
Irbid-Ramtha	4116	33.4	5.7	5.7	22.0	4.0
Jarash-Ajloun	1468	13.8	7.3	2.9	3.6	3.6
Mafraq	17,939	116.5	7.5	4.5	104.5	65.0
Balqaa	1079	9.4	4.0	3.2	2.2	2.0
Zarqa	6705	32.0	6.5	6.1	19.4	13.8
Amman-Madaba	13,100	71.3	12.9	3.9	54.5	36.7
Azraq	5280	38.6	2.7	–	35.9	16.4
Ghor As-Safi	5161	42.0	37.1	–	4.9	1.3
Karak-Tafileh	3348	15.2	9.2	1.4	4.6	4.8
Wadi Araba	1603	6.4	–	0.50	5.9	5.5
Jafr-Shoubak	6269	25.0	1.9	1.2	21.9	12.4
Quwayrah-Disi	3682	37.6	–	–	37.6	35.7
Total	98,135	702	298	29	375	235

* Including the flow from side wadis and springs and TWW for irrigated areas in JV. ** The figure includes amounts from Mukheiba wells which provided KAC with 16.7 MCM.

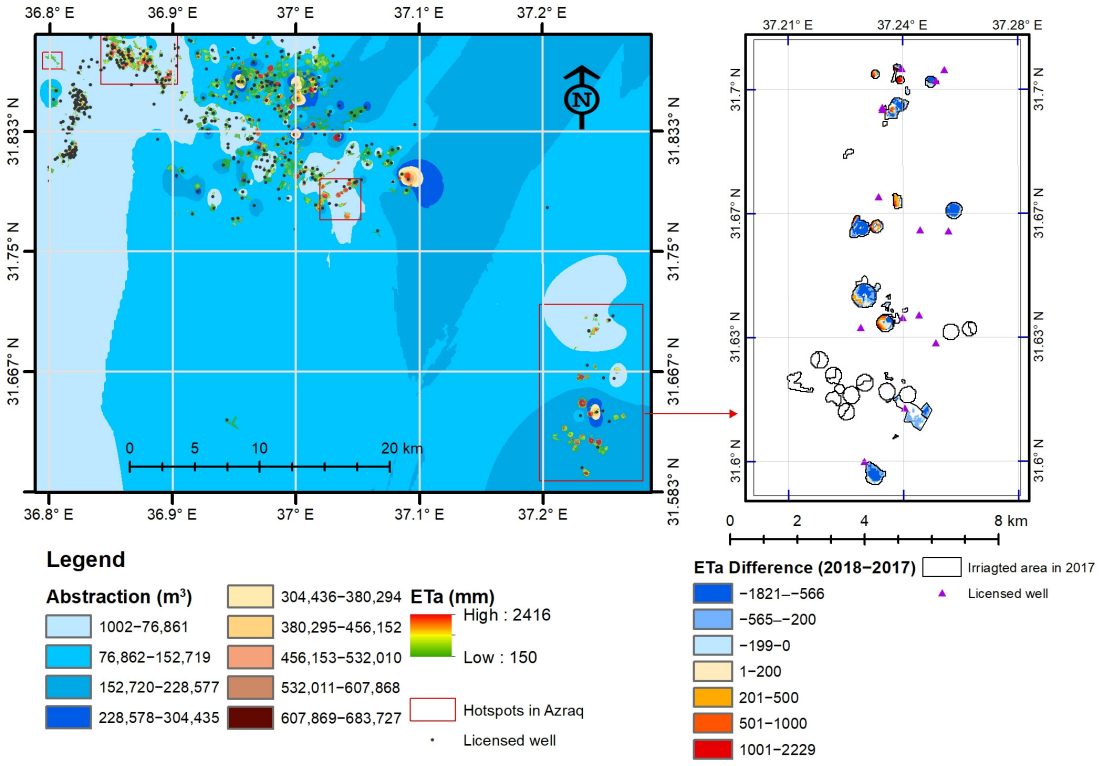

(**a**) (**b**)

Figure 13. Application of spatial analysis to identify hotspots with illegal access to water resources: an example from Azraq irrigated zone. (**a**) Overlay of groundwater abstraction map with the map of ET-density of 2017 to identify and delineate hotspots; (**b**) Analysis of changes in irrigated area and water consumption in the area of Hazeem after implementation of a campaign by MWI in 2018 to shutdown illegal wells.

Table 5. Summary of irrigated areas, IWC, and cropping patterns in the irrigated zones in Jordan during 2017–2019.

	Area (ha)					IWC (MCM)					Cropping Pattern (%)			
Zone	**Min. ***	**Max.**	**Mean**	**S.E.**	**C.L.**	**Min.**	**Max.**	**Mean**	**S.E.**	**C.L.**	**Vegetables**	**Trees**	**Mixed**	**Fodders and Cereals**
1- North JV	10,796	11,120	10,962	94	403	90.7	96.2	93.6	1.59	6.8	34.7	61.5	2.0	1.8
2- Middle-South JV	14,784	17,265	16,207	739	3180	157.2	168.3	163.3	3.26	14.0	71.3	26.4	1.3	1.0
3- Irbid-Ramtha	3769	4116	3974	105	452	29.3	33.4	31.8	1.27	5.4	83.9	14.3	0.4	1.3
4- Jarash-Ajloun	1401	1468	1431	20	84	13.8	14.9	14.2	0.34	1.5	25.6	53.9	18.9	1.7
5- Mafraq	17,939	18,596	18,243	191	823	101.5	118.2	112.1	5.31	22.8	32.1	62.0	4.9	1.0
6- Balqaa	1079	1185	1149	35	150	6.8	9.4	8.2	0.76	3.3	48.0	38.7	12.7	0.7
7- Zarqa	6131	6923	6586	236	1016	28.6	34.0	31.5	1.58	6.8	51.3	26.5	6.4	15.9
8- Amman-Madaba	12,530	13,100	12,820	165	708	67.0	71.3	69.2	1.24	5.3	54.2	36.3	6.0	3.5
9- Azraq	5004	5391	5225	115	495	38.6	45.3	42.1	1.94	8.3	20.3	38.4	18.7	22.5
10- Ghor As-Safi	5077	5161	5125	25	108	32.8	42.0	37.1	2.67	11.5	90.1	8.4	0.2	1.3
11- Karak-Tafileh	2786	3348	3072	162	698	15.2	16.5	15.9	0.38	1.7	48.7	17.5	22.2	11.6
12- Wadi Araba	1382	1603	1507	65	282	5.8	6.9	6.4	0.32	1.4	87.3	12.0	0.3	0.4
13- Jafr-Shoubak	6011	6429	6236	122	524	25.0	34.0	28.8	2.69	11.6	52.1	32.5	6.5	9.1
14- Quwayrah-Disi	3682	4122	3868	131	566	36.8	43.7	39.4	2.18	9.4	55.0	22.1	10.2	12.7
Jordan	95,295	98,135	96,407	876	3768	688	702	694	4.26	18.3				

* Min. = minimum, Max. = maximum, S.E. = standard error, C.L. = confidence level (95%).

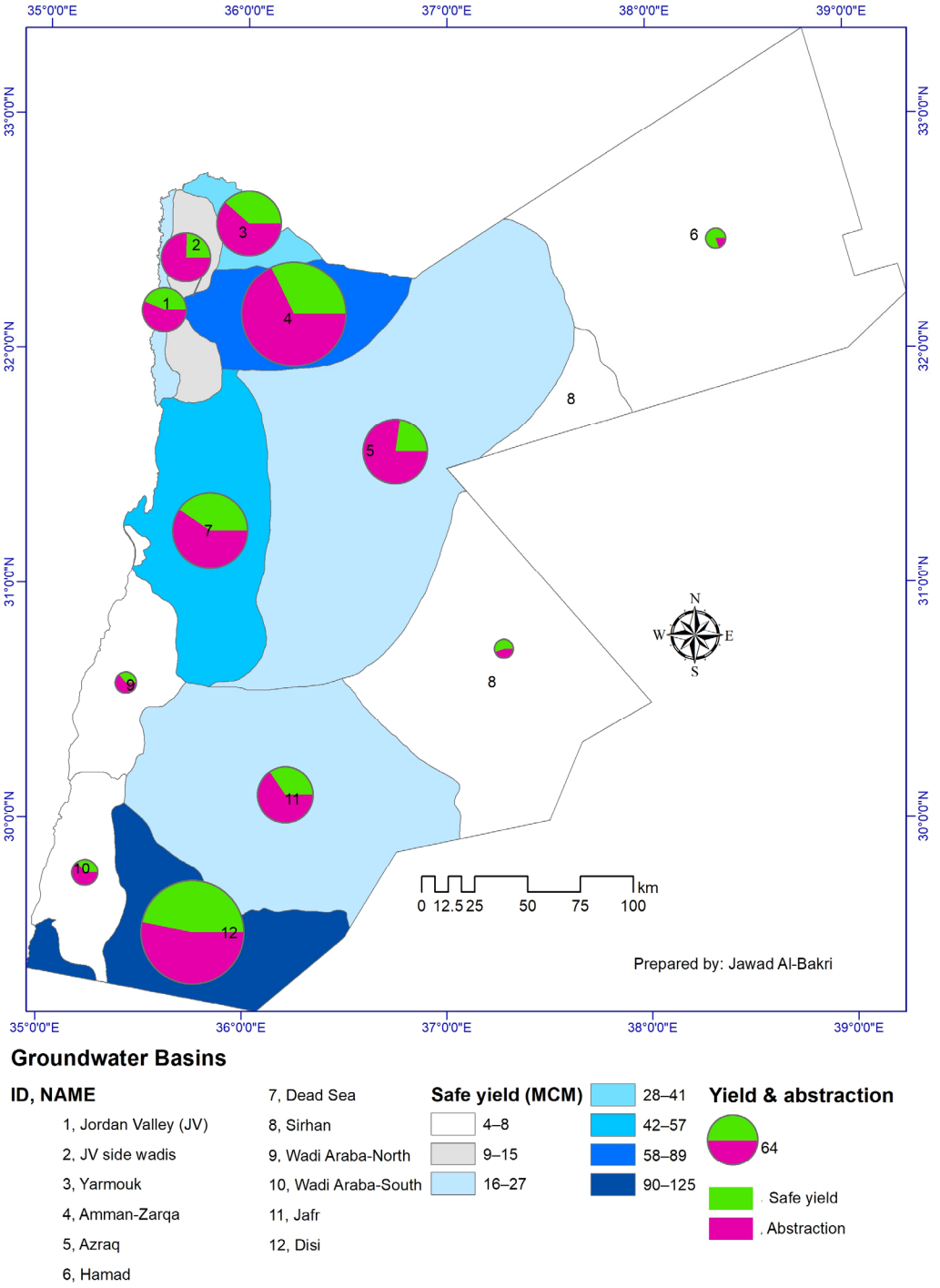

Figure 14. Groundwater basins in Jordan with levels of abstraction and safe yield.

3.5. Historical Changes and Future Trends of Irrigated Areas and IWC

Results showed an obvious expansion in irrigation during 1987–2019, with a relatively higher rate of change during 1987–2002 compared to 2002–2019. Prediction of future irrigated lands showed that the irrigated area would reach 137 thousand ha by 2050 if the same trends of expansion would continue (Table 6). The zones which would have significant expansions in irrigation would be Irbid-Ramtha, Amman-Madaba, and JV. In these zones, the expansion would be mainly attributed to the increased amounts of TWW. Expansion of irrigation in the desert areas (Mafraq, Azraq, Jafr) would put more pressure on the existing fragile and over-pumped groundwater resources. Therefore, deep aquifers of groundwater might be used by farmers to meet demands on food. Due to limitations of

data on historical cropping patterns and irrigation efficiency, historical IWC values were calculated assuming similar cropping patterns and levels of ET. Subsequently, the historical IWC was estimated at 390 MCM and 528 MCM in the years 1987 and 2002, respectively. The future water demand would be 849 MCM in 2034 and 986 MCM in 2050.

Table 6. Summary of irrigated areas (ha) in Jordan during 1987–2019 and in the future.

Zone	Year 1987	Year 2002	Year 2018	Year 2034	Year 2050
Jordan Valley	26,294	30,274	25,580	30,580	36,580
Irbid-Ramtha	1159	1200	4038	7191	11,247
Jarash-Ajloun	930	1121	1401	1681	1913
Mafraq	4085	10,621	18,596	22,315	23,803
Balqaa	816	983	1185	1386	2253
Zarqa	1875	3954	6923	8308	9452
Amman-Madaba	4076	6827	12,829	15,908	19,252
Azraq	1690	3460	5391	6847	8135
Ghor As-Safi	5081	5081	5077	5081	5081
Karak-Tafileh	2174	2589	3082	3575	3966
Wadi Araba	359	704	1382	2061	2790
Jafr-Shoubak	1039	2498	6011	9524	9500
Quwayrah-Disi	4847	4292	3800	3800	3800
Total	54,625	73,804	95,295	118,637	137,771

4. Discussion

4.1. Remotely Sensed Irrigation Maps

The study showed that maps derived from digital classification of multi-temporal NDVI layers enabled the accurate mapping of irrigated crops. The levels of mapping accuracy varied among the different climatic regions, with relatively higher accuracy of mapping for irrigated areas in desert areas than in JV and the Mediterranean highlands. The levels of mapping accuracy were in agreement with results reported by previous studies in Jordan [43,70]. The study showed that different methods could be used for mapping irrigated areas. The levels of accuracy would improve by the use of ancillary data which might include locations of groundwater wells and water sources, irrigated farm units and cropping patterns, and observations from ground surveys.

In general, the method of density slicing of the annual sum of NDVI layers was able to detect irrigated farms in the desert areas of Jafr-Shoubak and Quwayrah-Disi with high accuracy. In both zones, irrigated areas with an NDVI annual sum of 3.0 and above represented irrigated areas. An annual NDVI sum of 13 and above represented irrigated areas cultivated with alfalfa. In Mafraq, the method of mapping which enabled the separation of irrigated and rainfed crops included the use of the maximum NDVI during May-November and knowledge-based classification that utilized ranges of NDVI during the growing seasons. The irrigated areas with long growing seasons were classified into two groups of NDVI-maximum (0.31–0.49 and 0.50–1.00), while vegetable crops with a short growing season were characterized by a lower NDVI-maximum (0.20–0.30). The method of unsupervised classification (ISODATA) for NDVI multi-temporal layers was able to detect and classify irrigated areas in JV and the Mediterranean highlands. In JV irrigated areas, Sentinel-2 images were needed to separate citrus from vegetable crops and cereals. In the highlands, the use of SEBAL-ET layers for March-October was needed to refine classification results and to improve classification accuracy.

In terms of total irrigated areas, results from this study were compared with figures reported from detailed land cover mapping carried out by the Food and Agriculture Organization of the United Nations (FAO) [70] and data of DOS [61]. The work of FAO used an Object-Based Image Analysis (OBIA) of multi-temporal Sentinel-2 layers of vegetation indices (Ratio Vegetation Index (RVI) and NDVI). Results of FAO showed that the total irrigated area in Jordan in 2019 reached 1068 thousand ha, with an overall mapping accuracy of 88–94%. The area of irrigated crops, reported by FAO, is quite close to the figure obtained

by this study (981 thousand ha in 2019). The differences in both figures could be attributed to the methods of classification, remote sensing data, and the classification scheme. In this study, the classification scheme included five categories of irrigated crops, while the study of FAO included two categories of irrigated crops: orchards and vegetables.

Comparing the study results with data of DOS [61] showed that irrigated areas obtained from this study were higher than the areas reported by DOS. According to DOS, the total irrigated areas in Jordan were 86 thousand ha in 2017, 84 thousand ha in 2018, and 80 thousand ha in 2019. These figures are less than the results obtained in this study and the study of FAO [70]. The variations between DOS figures and our study could be attributed to the fact that DOS figures were based on statistical methods of sampling that included structured interviews with farmers, while remote sensing methods used in this study had the strength of spatial dimension that covered the whole country. This fact was supported by the total area of landholdings where irrigation was practiced. The figure obtained from this study showed that the total area of lands where irrigation was practiced during 2017–2019 was 133 thousand ha. This area was slightly higher than the 122 thousand ha reported by DOS for the year 2017.

4.2. Remote Sensing of ET and IWC

Outputs from ET mapping showed that remotely sensed ET from SEBAL and its NDVI-Kc-derived relationships were useful in studying the spatial dimension of ET and in providing solid and accurate figures on IWC. The approach of converting ET to IWC, however, would require ground data on water delivered to farmers, as in the cases of JV and the highlands. The derived relationships of NDVI-Kc were significant and were in agreement with previous studies carried out in different agro-climatological zones [21,71,72]. Therefore, the NDVI-Kc relationships would be highly beneficial to derive ET maps for large irrigation schemes. Furthermore they could be used to schedule irrigation at the farm level [73], particularly in areas where no weather data would be available. In the context of Jordan, the contribution of ET mapping through NDVI-Kc and SEBAL will be the improvement of IWC estimates used in the annual reports of Jordan's water budget, as remote-sensing-based ET will provide the actual data for all the irrigated areas in Jordan. The country-wide remote sensing assessment reported in this study, which confirmed findings of a previous study [74], concluded that illegal groundwater abstractions were much higher than the figures reported by the MWI.

Outputs from ET mapping could also be used to assess the levels of irrigation efficiency in Jordan. This could be obtained from the conversion factor between remotely sensed ET and IWC (Appendix B), which was the range of 0.60 to 0.76. This range is in agreement with results reported for JV [75], where the overall efficiency of application and conveyance is 65%. The level of irrigation efficiency in th highlands is also in agreement with groundwater assessment in Jordan [76], which shows observed substantial decline in groundwater levels exacerbated by increased abstraction to address the increased water demand.

The contribution of RS to AWM was indicated by the results of this study, which showed that ET estimates of IWC were higher than MWI estimates. The difference between RS estimates and MWI figures was 140 MCM, indicating high levels of IWC and groundwater depletion in the country (Figure 14). The implications of this figure would be the possible solutions for water scarcity. Although insufficiencies in water supply would be seen as main factors that contributed to water scarcity in the country [46,47], empowerment of water auditing and monitoring would contribute to water governance by reducing the non-revenue water [45]. Results from this study emphasized the use of RS as part of AI and smart water management systems. Analysis of ET and irrigated crops would show hotspots with high water consumption.

4.3. Future Planning of Irrigated Agriculture

Outputs from this study reflected the important contribution of remote sensing in predicting changes in irrigated areas, while considering available water resources in each

irrigated zone. The use of remotely sensed ET and maps of irrigated crops aided in identifying irrigated zones that consumed most of the irrigation water in Jordan. These were JV, Mafraq, JV, and Amman-Madaba. During 2019, the zones of JV and Mafraq consumed 54% of irrigation water in Jordan. In terms of groundwater consumption, the irrigated area of Mafraq consumed 28% of the total groundwater used in irrigation. Such information would be crucial for planning water allocation in the future, as expansion in irrigated agriculture would enable MWI to develop additional water resources for irrigation. In JV, expansion of the irrigated area would be possible, as the present TWW effluent of 178 MCM would increase to 250 MCM in 2025 and would double by 2050 [77]. Most of TWW would be disposed to KTD and other reservoirs on the side wadis of JV. Therefore, expansion in irrigation would be possible in the highlands where TWW would be available and in MSJV, as well.

The use of remote sensing to predict irrigated areas and their IWC was important to identify levels of water deficit in Jordan. Considering that 140 MCM of groundwater 2qw over-abstracted in 2019, the total deficit would reach 422 MCM. A considerable part of this deficit (about 300 MCM) will be compensated by TWW, while other sources shall be investigated to compensate the remaining part of this deficit. An environmental assessment showed that the reuse of TWW would also have positive impacts on groundwater depletion with annual savings of 72.6 MCM [78]. At present, decentralized TWW is not fully or efficiently utilized, while centralized WWTP would require expansion to receive an additional influent of 5% per year [69]. The increased volumes of TWW will come from domestic areas which will receive 350 MCM of water from the national desalination project, expected to operate in 2027. These findings, in addition to the remote sensing assessment presented in this study, were included in the new Water Master Plan (WMP) of Jordan [79], which introduced, for the first time, a detailed water balance, including the forecast for surface and groundwater resources over the planning horizon until 2040.

5. Conclusions

The study showed how remote sensing data from earth observation systems (EOSs) could be used to provide spatial maps and information needed for AWM under scarce water conditions. The methods of the unsupervised classification, density slicing NDVI, and the knowledge-based classifier provided accurate maps for irrigated crops. The methods of crop mapping emphasized the integration of remote sensing images of Landsat 8 and Sentinel-2 with the ground data and ET maps to obtain accurate maps for irrigated crops. The study developed relationships between NDVI and Kc to derive ET and to accurately map IWC. The advantages of using these relationships over other remote-sensing-based models were the rapid mapping of ET and the fact that they did not require hourly climatic records, which were not available for all irrigated zones. Therefore, it is recommended to use the methods developed by this study for the mapping of irrigated areas and ET. The study indicated the important contribution of these methods to the AWM. Using these methods would provide accurate estimates for the present consumption and the future demand of irrigation water. In terms of water governance, the use of remote sensing methods would provide estimates for non-revenue water and would increase water savings. Furthermore, they would provide maps for locations where incorrect metering of groundwater abstraction or illegal access to a water source might exist. In terms of AWM in Jordan, the study showed that levels of IWC were high when compared with the safe yield of groundwater and the available water resources in the country. Finally, the study recommends the adoption of zoning followed for assessing IWC for the irrigated areas in Jordan, as it will enable better planning of water supply and demand, which will contribute to AWM in the country.

Author Contributions: Conceptualization, J.T.A.-B.; methodology, J.T.A.-B., G.D. and A.C.; software, J.T.A.-B. and E.A.; mapping and validation, J.T.A.-B. and E.A.; field visits, J.T.A.-B., M.A. and E.A.; formal analysis, J.T.A.-B., G.D., A.C., M.A. and A.M..; investigation, J.T.A.-B., G.D., A.C. and A.M.; resources, A.M. and M.A.; climatic data curation, J.T.A.-B. and E.A.; writing—original draft

preparation, J.T.A.-B., G.D. and A.C.; writing—review and editing, all authors; visualization, J.T.A.-B. and G.D. All authors have read and agreed to the published version of the manuscript.

Funding: This research carried out through two international agencies that support water sector in Jordan. The work of crop and ET mapping for five groundwater basins of highlands during 2017 and 2018 was funded by the United States Agency for International Development (USAID) within the activities of Water Management Initiative (MWI) which was implemented by Orient Engineering Consultancy and Tetra Tech (Contract No. AID-278-C-16-00001). The work of crop and ET mapping for Jordan Valley during 2017 and 2018 and for Jordan during 2019 was funded and carried outs as part of the GIZ Water Program project "Management of Water Resources (MWR)" (PN 2018.2226.1). The project is part of German Technical Assistance to Jordan and was included as part of Jordan's Third National Water Master Plan (NWMP-3). The work of SEBAL-ET and land-use/cover mapping for Jordan Valley was carried out through FAO-RNE (Implementing the Agenda 2030 on water efficiency/productivity and sustainability in the NENA region, Water Scarcity Initiative (WSI), funded by SIDA, GCP/RNE/009/SWE) and ERANETMED EO-TIME (Earth Observation Technologies for Irrigation in Mediterranean Environment), Italian Ministry University and Research, Decree no.1768/2019.

Data Availability Statement: Data on water resources for 2017–2019 is available (Arabic version) through the MWI website http://www.mwi.gov.jo/ (accessed on 28 November 2022). Maps of irrigated crops and water consumption are archived at MWI, USAID-MWI and GIZ, with detailed results in soft and hardcopy reports.

Acknowledgments: The authors acknowledge the cooperation of the MWI and the agencies that supported the work. In particular, deep appreciation and acknowledgements are extended to Engineers Awni Kloub and Adel Alobeiaat (MWI), Eng. Saddam Khleifat (Orient Engineering Consultancy), Jose A. Valdez Novillo (Tetra Tech), Hala Shahin and Ahmad Abu Hijleh (GIZ). The authors also acknowledge the anonymous reviewers who improved the quality of this article.

Conflicts of Interest: The authors declare no conflict of interest.

Appendix A

Table A1. Examples of Landsat 8 images used for mapping irrigated crops in 2018 and sum of ETr (mm) for the main irrigated area covered by each image.

No.	Date—DD/MM/YYYY	173/038 Azraq	173/039 Jafr	173/040 Disi	Date—DD/MM/YYYY	174/037 NJV	174/038 Amman	174/039 Wadi Araba
1.	16 January 2018	Cloudy *	40.9	54.21	7 January 2018	7.5	9.1	16.6
2.	1 February 2018	90.4	45.8	54.52	23 January 2018	31.5	Cloudy **	Cloudy *
3.	17 February 2018	Cloudy *	Cloudy *	Cloudy *	8 February 2018	Cloudy **	Cloudy **	Cloudy *
4.	5 March 2018	143.5	101.0	166.72	24 February 2018	57.8	94.8	157.0
5.	21 March 2018	138.3	99.9	121.42	12 March 2018	42.6	50.1	81.51
6.	6 April 2018	136.4	97.8	138.9	28 March 2018	Cloudy *	Cloudy *	Cloudy *
7.	22 April 2018	141.8	Cloudy *	137.78	13 April 2018	132.6	171.8	206.0
8.	8 May 2018	Cloudy *	213.5	137.72	29 April 2018	72.7	93.3	116.1
9.	24 May 2018	328.5	Cloudy *	186.91	15 May 2018	90.9	103.5	143.1
10.	9 June 2018	200.5	269.0	169.45	31 May 2018	Cloudy *	Cloudy *	Cloudy *
11.	25 June 2018	232.1	138.3	190.1	16 June 2018	195.2	276.1	345.1
12.	11 July 2018	242.1	128.1	192.8	2 July 2018	109.6	125.5	177.6
13.	27 July 2018	224.2	151.7	180.2	18 July 2018	104.0	141.8	170.2
14.	12 August 2018	242.2	119.8	174.6	3 August 2018	Cloudy *	131.2	Cloudy *
15.	28 August 2018	197.6	103.3	166.5	19 August 2018	220.7	116.5	326.6

Table A1. *Cont.*

No.	Date—DD/MM/YYYY	173/038 Azraq	173/039 Jafr	173/040 Disi	Date—DD/MM/YYYY	174/037 NJV	174/038 Amman	174/039 Wadi Araba
16.	13 September 2018	192.2	Cloudy *	Cloudy *	4 September 2018	93.9	108.8	156.2
17.	29 September 2018	150.1	173.8	298.6	20 September 2018	88.7	94.9	131.8
18.	15 October 2018	138.8	85.5	113.5	6 October 2018	62.0	81.9	Cloudy *
19.	31 October 2018	129.8	60.2	Cloudy *	22 October 2018	44.6	60.7	214.3
20.	16 November 2018	Cloudy *	39.9	187.2	7 November 2018	81.8	98.8	122.7
21.	2 December 2018	125.4	Cloudy *	Cloudy *	23 November 2018	Cloudy **	Cloudy **	Cloudy **
22.	18 December 2018	73.8	68.8	144.0	9 December 2018	73.6	71.9	Cloudy **
23.	N/A				25 December 2018	36.3	37.3	161.5
Annual Total		3129	1937	2815		1546	1868	2526
Other irrigated areas covered by the image		Mafraq	Disi	Jafr		Irbid-Ramtha	Zarqa, MSJV	Karak -Tafileh

* Replaced by Landsat 7. ** Outside the irrigation seasons.

Appendix B

Table A2. List of conversion factors of SEBAL-ET- and NDVI-Kc-derived ET to IWC with examples of sample locations used for deriving the conversion factor.

Zone	ET-IWC Conversion Factor	Crop (s)	Exmples on Locations (s)	
			Longitude (°E)	Latitude (°N)
1- North JV	0.76	Citrus	35.5707	32.4269
		Tomato	35.6091	32.4456
		Banana	35.5850	32.3956
2- Middle-South JV	0.70	Date palm	35.5965	32.0900
		Tomato	35.5982	32.1235
3- Irbid-Ramtha	0.65	Potato,	35.9531	32.5447
		Mixed cropping	35.9616	32.5546
		Alfalfa	35.9857	32.5947
4- Jarash-Ajloun	0.70	Fruit trees	35.6811	32.3010
		Vegetables	35.9962	32.2403
5- Mafraq	0.74	Fruit trees (peaches)	36.4825	32.3268
		Olives	36.2896	32.3461
		Alfalfa	36.4582	32.2798
6- Balqaa	0.70	Vegetables, fruit trees	35.8230	32.0722
7- Zarqa	0.68	Alfalfa	36.3958	32.1399
		Vegetables	36.5664	32.0425
		Fruit trees	36.4108	32.0704
8- Amman-Madaba	0.75	Olives	36.0418	31.7448
		Fruit trees	36.0271	31.6282
		Alfalfa	35.8061	31.6915
9- Azraq	0.64	Fruit trees	36.9209	31.8374
		Vegetables	36.9224	31.8812
		Date palm	36.8004	31.8065
		Barley	36.9572	31.8412
10- Ghor As-Safi	0.72	Tomato	35.4441	30.9120
		Fruit trees	35.5098	31.2830

Table A2. *Cont.*

Zone	ET-IWC Conversion Factor	Crop (s)	Exmples on Locations (s)	
			Longitude (°E)	Latitude (°N)
11- Karak-Tafileh	0.75	Olives	35.6070	30.8420
		Alfalfa	35.4415	30.4111
12- Wadi Araba	0.60	Tomato	35.3908	30.6319
		Water melon	35.3736	30.5775
13- Jafr-Shoubak	0.60	Apples	35.5855	30.4537
		Vegetables	35.7478	30.4332
14- Quwayrah-Disi	0.62	Vegetables	35.5533	29.6314
		Alfalfa	35.5953	29.6110
		Date palm	35.3274	29.7410

References

1. Srivastava, P.K.; Suman, S.; Pandey, V.; Gupta, M.; Gupta, A.; Gupta, D.K.; Chaudhary, S.K.; Singh, U. Concepts and methodologies for agricultural water management. In *Agricultural Water Management: Theories and Practices*; Srivastava, P.K., Gupta, M., Tsakiris, G., Quinn, N.W., Eds.; Academic Press: London, UK, 2021; pp. 1–18.
2. Dube, T.; Shekede, M.D.; Massari, C. Remote sensing for water resources and environmental management. *Remote Sens.* **2023**, *15*, 18. [CrossRef]
3. Sonneveld, B.G.J.S.; Merbis, M.D.; Alfarra, A.; Ünver, O.; Arnal, M.A. *Nature-Based Solutions for Agricultural Water Management and Food Security, FAO Land and Water Discussion Paper 12*; Food and Agriculture Organization of the United Nations (FAO): Rome, Italy, 2018; p. 66. Available online: https://www.fao.org/3/ca2525en/ca2525en.pdf (accessed on 28 November 2022).
4. FAO. *The State of Food and Agriculture 2020: Overcoming Water Challenges in Agriculture*; Food and Agriculture Organization of the United Nations (FAO): Rome, Italy, 2020; p. 210. Available online: https://doi.org/10.4060/cb1447en (accessed on 28 November 2022). [CrossRef]
5. Basukala, A.K.; Oldenburg, C.; Schellberg, J.; Sultanov, M.; Dubovyk, O. Towards improved land use mapping of irrigated croplands: Performance assessment of different image classification algorithms and approaches. *Eur. J. Remote Sens.* **2017**, *50*, 187–201. [CrossRef]
6. Thakur, R.; Manekar, V.L. Artificial intelligence-based image classification techniques for hydrologic applications. *Appl. Artif. Intell.* **2022**, *36*, 187–201. [CrossRef]
7. Lowe, M.; Qin, R.; Mao, X. A Review on Machine Learning, Artificial Intelligence, and Smart Technology in Water Treatment and Monitoring. *Water* **2022**, *14*, 1384. [CrossRef]
8. Krishnan, S.R.; Nallakaruppan, M.K.; Chengoden, R.; Koppu, S.; Iyapparaja, M.; Sadhasivam, J.; Sethuraman, S. Smart Water Resource Management Using Artificial Intelligence—A Review. *Sustainability* **2022**, *14*, 13384. [CrossRef]
9. Cai, X.; Rosegrant, M.W. Global water demand and supply projections. *Water Int.* **2002**, *27*, 159–169. [CrossRef]
10. Mancosu, N.; Snyder, R.L.; Kyriakakis, G.; Spano, D. Water scarcity and future challenges for food production. *Water* **2015**, *7*, 975–992. [CrossRef]
11. Serbina, L.; Miller, H.M. *Landsat and Water—Case Studies of the Uses and Benefits of Landsat Imagery in Water Resources*; U.S. Geological Survey Open-File Report 2014–1108; U.S. Geological Survey: Reston, VA, USA, 2014; p. 61. [CrossRef]
12. Allen, R.G.; Pereira, L.A.; Raes, D.; Smith, M. *Crop Evapotranspiration—Guidelines for Computing Crop Water Requirements; FAO Irrigation and Drainage Paper 56*; Food and Agriculture Organization of the United Nations (FAO): Rome, Italy, 1998; Available online: http://www.fao.org/3/X0490E/x0490e00.htm (accessed on 10 September 2022).
13. Pereira, L.S.; Allen, R.G.; Smith, M.; Raes, D. Crop evapotranspiration estimation with FAO56: Past and future. *Agric. Water Manag.* **2015**, *147*, 4–20. [CrossRef]
14. Nassar, A.; Torres-Rua, A.; Kustas, W.; Nieto, H.; McKee, M.; Hipps, L.; Stevens, D.; Alfieri, J.; Prueger, J.; Alsina, M.M.; et al. Influence of model grid size on the estimation of surface fluxes using the two source energy balance model and sUAS imagery in vineyards. *Remote Sens.* **2020**, *12*, 342. [CrossRef]
15. Garrido-Rubio, J.; Calera, A.; Arellano, I.; Belmonte, M.; Fraile, L.; Ortega, T.; Bravo, R.; González-Piqueras, J. Evaluation of remote sensing-based irrigation water accounting at river basin district management scale. *Remote Sens.* **2020**, *12*, 3187. [CrossRef]
16. Drexler, J.Z.; Snyder, R.L.; Spano, D.; Paw U, K.T. A review of models and micrometeorological methods used to estimate wetland evapotranspiration. *Hydrol. Process.* **2004**, *18*, 2071–2101. [CrossRef]
17. Calera, A.; Campos, I.; Osann, A.; D'Urso, G.; Menenti, M. Remote sensing for crop water management: From ET modelling to services for the end users. *Sensors* **2017**, *17*, 1104. [CrossRef]
18. Anderson, M.C.; Kustas, W.P.; Norman, J.M.; Hain, C.R.; Mecikalski, J.R.; Schultz, L.; González-Dugo, M.P.; Cammalleri, C.; D'urso, G.; Pimstein, A.; et al. Mapping daily evapotranspiration at field to continental scales using geostationary and polar orbiting satellite imagery. *Hydrol. Earth Syst. Sci.* **2011**, *15*, 223–239. [CrossRef]

19. Allen, R.G.; Tasumi, M.; Trezza, R. Satellite-based energy balance for mapping evapotranspiration with internalized calibration (METRIC)—Model. *J. Irrig. Drain. Eng.* **2007**, *133*, 380–394. [CrossRef]
20. Bastiaanssen, W.G.M.; Menenti, M.; Feddes, R.A.; Holtslag, A.A.M. A remote sensing surface energy balance algorithm for land (SEBAL). 1. Formulation. *J. Hydrol.* **1998**, *212–213*, 198–212. [CrossRef]
21. Campos, I.; Neale, C.M.U.; Calera, A.; Balbontín, C.; González-Piqueras, J. Assessing satellite-based basal crop coefficients for irrigated grapes (*Vitis vinifera* L.). *Agric. Water Manag.* **2010**, *98*, 45–54. [CrossRef]
22. FAO. *WaPOR Database Methodology: Version 2 Release*; FAO: Rome, Italy, 2020; p. 90. [CrossRef]
23. Grosso, C.; Manoli, G.; Martello, M.; Chemin, Y.H.; Pons, D.H.; Teatini, P.; Piccoli, I.; Morari, F. Mapping Maize Evapotranspiration at Field Scale Using SEBAL: A Comparison with the FAO method and soil-plant model simulations. *Remote Sens.* **2018**, *10*, 1452. [CrossRef]
24. Wagle, P.; Gowda, P.H. Editorial for the Special Issue "Remote Sensing of evapotranspiration (ET)". *Remote Sens.* **2019**, *11*, 2146. [CrossRef]
25. Jung, H.C.; Getirana, A.; Arsenault, K.R.; Holmes, T.R.H.; McNally, A. Uncertainties in evapotranspiration estimates over West Africa. *Remote Sens.* **2019**, *11*, 892. [CrossRef]
26. Dhungel, S.; Barber, M.E. Estimating calibration variability in evapotranspiration derived from a satellite-based energy balance model. *Remote Sens.* **2018**, *10*, 1695. [CrossRef]
27. Nassar, A.; Torres-Rua, A.; Kustas, W.; Alfieri, J.; Hipps, L.; Prueger, J.; Nieto, H.; Alsina, M.M.; White, W.; McKee, L.; et al. Assessing daily evapotranspiration methodologies from one-time-of-day sUAS and EC information in the *GRAPEX* project. *Remote Sens.* **2021**, *13*, 2887. [CrossRef] [PubMed]
28. Asadi, M.; Kamran, K.V. Comparison of SEBAL, METRIC, and ALARM algorithms for estimating actual evapotranspiration of wheat crop. *Theor. Appl. Climatol.* **2022**, *149*, 327–337. [CrossRef]
29. Chen, Y.; Xia, J.; Liang, S.; Feng, J.; Fisher, J.B.; Li, X.; Li, X.; Liu, S.; Ma, Z.; Miyata, A.; et al. Comparison of satellite-based evapotranspiration models over terrestrial ecosystems in China. *Remote Sens. Environ.* **2014**, *140*, 279–293. [CrossRef]
30. Singh, R.K.; Senay, G.B. Comparison of Four different energy balance models for estimating evapotranspiration in the Midwestern United States. *Water* **2016**, *8*, 9. [CrossRef]
31. Allen, R.; Irmak, A.; Trezza, R.; Hendrickx, J.M.H.; Bastiaanssen, W.; Kjaersgaard, J. Satellite-based ET estimation in agriculture using SEBAL and METRIC. *Hydrol. Process.* **2011**, *25*, 4011–4027. [CrossRef]
32. Suleiman, A.; Bali, K.M.; Kleissl, J. Comparison of ALARM and SEBAL Evapotranspiration of Irrigated Alfalfa. In Proceedings of the ASABE Annual International Meeting, Reno, Nevada, 21–24 June 2009. [CrossRef]
33. Owaneh, O.M.; Suleiman, A.A. Comparison of the performance of ALARM and SEBAL in estimating the actual daily ET from satellite data. *J. Irrigat. Drain. Eng.* **2018**, *144*, 04018024. [CrossRef]
34. Zhou, X.; Bi, S.; Yang, Y.; Tian, F.; Ren, D. Comparison of ET estimations by the three-temperature model, SEBAL model and eddy covariance observations. *J. Hydrol.* **2014**, *519*, 769–776. [CrossRef]
35. Rahimzadegan, M.; Janani, A. Estimating evapotranspiration of pistachio crop based on SEBAL algorithm using Landsat 8 satellite imagery. *Agr. Water Manag.* **2019**, *217*, 383–390. [CrossRef]
36. Liou, Y.-A.; Kar, S.K. Evapotranspiration Estimation with Remote Sensing and Various Surface Energy Balance Algorithms—A Review. *Energies* **2014**, *7*, 2821–2849. [CrossRef]
37. Acharya, B.; Sharma, V. Comparison of satellite driven surface energy balance models in estimating crop evapotranspiration in semi-arid to arid inter-mountain region. *Remote Sens.* **2021**, *13*, 1822. [CrossRef]
38. Jaafar, H.H.; Ahmad, F.A. Time series trends of Landsat-based ET using automated calibration in METRIC and SEBAL: The Bekaa Valley, Lebanon. *Remote Sens.* **2020**, *238*, 111034. [CrossRef]
39. Hlavaty, H. *Water Management Initiative: Review of Water Scarcity Ranking Methodologies. A Report Prepared for Tetra Tech*; USAID Water Management Initiative (WMI): Amman, Jordan, 2018.
40. MWI (Ministry of Water and Irrigation, Jordan). *Water Budget for Year 2017*; Department of Policies and Strategic Planning, Ministry of Water and Irrigation: Amman, Jordan, 2018.
41. MWI (Ministry of Water and Irrigation, Jordan). *Water Budget for Year 2018*; Department of Policies and Strategic Planning, Ministry of Water and Irrigation: Amman, Jordan, 2019.
42. MWI (Ministry of Water and Irrigation, Jordan). *Water Budget for Year 2019*; Department of Policies and Strategic Planning, Ministry of Water and Irrigation: Amman, Jordan, 2020.
43. Al-Bakri, J.T.; Shawash, S.; Ghanim, A.; Abdelkhaleq, R. Geospatial techniques for improved water management in Jordan. *Water* **2016**, *8*, 132. [CrossRef]
44. WMI (Water Management Initiative). *Remote Sensing for Crop Mapping and Assessment for Groundwater Abstraction in Azraq Basin*; A report by Tetra Tech for USAID; USAID: Amman, Jordan, 2020. Available online: https://pdf.usaid.gov/pdf_docs/PA00X8QM.pdf (accessed on 20 October 2022).
45. Yorke, V. Jordan's shadow state and water management: Prospects for water security will depend on politics and regional cooperation. In *Society–Water–Technology. A Critical Appraisal of Major Water Engineering Projects*; Hüttl, R.F., Bismuth, O.B.C., Hoechstetter, S., Eds.; Springer: Cham, Switzerland, 2016; pp. 227–251. Available online: https://doi.org/10.1007/978-3-319-18971-0_15 (accessed on 28 November 2022). [CrossRef]
46. Hussein, H. Lifting the veil: Unpacking the discourse of water scarcity in Jordan. *Environ. Sci. Policy* **2018**, *89*, 385–392. [CrossRef]

47. Hussein, H. Tomatoes, tribes, bananas, and businessmen: An analysis of the shadow state and of the politics of water in Jordan. *Environ. Sci. Policy* **2018**, *84*, 170–176. [CrossRef]
48. Klauer, B.; Küblböck, K.; Omann, I.; Karutz, R.; Klassert, C.; Zhu, Y.; Zozmann, H.; Smilovic, M.; Talozi, S.; Figueroa, A.J.; et al. Stakeholder Workshops Informing System Modeling—Analyzing the Urban Food–Water–Energy Nexus in Amman, Jordan. *Sustainability* **2022**, *14*, 11984. [CrossRef]
49. Zozmann, H.; Klassert, C.; Sigel, K.; Gawel, E.; Klauer, B. Commercial Tanker Water Demand in Amman, Jordan—A Spatial Simulation Model of Water Consumption Decisions under Intermittent Network Supply. *Water* **2019**, *11*, 254. [CrossRef]
50. Al Naber, M.; Molle, F. Controlling groundwater over abstraction: State policies vs. local practices in the Jordan highlands. *Water Policy* **2017**, *19*, 692–708. [CrossRef]
51. Markham, B.; Storey, J.; Morfitt, R. Landsat-8 sensor characterization and calibration. *Remote Sens.* **2015**, *7*, 2279–2282. [CrossRef]
52. Drusch, M.; Del Bello, U.; Carlier, S.; Colin, O.; Fernandez, V.; Gascon, F.; Hoersch, B.; Isola, C.; Laberinti, P.; Martimort, P.; et al. Sentinel-2: ESA's optical high-resolution mission for GMES operational services. *Remote Sens. Environ.* **2012**, *120*, 25–36. [CrossRef]
53. ESA (European Space Agency). Sentinel-2 Mission, ESA. Available online: https://sentinel.esa.int/web/sentinel/missions/sentinel-2. (accessed on 2 September 2022).
54. Al-Bakri, J.T.; D'Urso, G.; Batchelor, C.; Abukhalaf, M.; Alobeiaat, A.; Al-Khreisat, A.; Vallee, D. Remote Sensing-Based Agricultural Water Accounting for the North Jordan Valley. *Water* **2022**, *14*, 1198. [CrossRef]
55. Ozdogan, M.; Yang, Y.; Allez, G.; Cervantes, C. Remote Sensing of Irrigated Agriculture: Opportunities and Challenges. *Remote Sens.* **2010**, *2*, 2274–2304. [CrossRef]
56. Jensen, J.R. *Introductory Digital Image Processing: A Remote Sensing Perspective (Pearson Series in Geographic Information Science)*, 4th ed.; Prentice Hall: Upper Saddle River, NJ, USA, 2015.
57. Simonneaux, V.; Duchemin, B.; Helson, D.; Raki, E.; Olioso, A.; Chehbouni, A. The use of high-resolution image time series for crop classification and evapotranspiration estimate over an irrigated area in central Morocco. *Int. J. Remote Sens.* **2008**, *29*, 95–116. [CrossRef]
58. El-Magd, I.A.; Tanton, T.W. Improvements in land use mapping for irrigated agriculture from satellite sensor data using a multi-stage maximum likelihood classification. *Int. J. Remote Sens.* **2003**, *24*, 4197–4206. [CrossRef]
59. Pontius Jr, R.G.; Millones, M. Death to Kappa: Birth of quantity disagreement and allocation disagreement for accuracy assessment. *Int. J. Remote Sens.* **2011**, *32*, 4407–4429. [CrossRef]
60. Foody, G.M. Explaining the unsuitability of the kappa coefficient in the assessment and comparison of the accuracy of thematic maps obtained by image classification. *Remote Sens. Environ.* **2020**, 111630. [CrossRef]
61. DOS (Department of Statistics, Jordan). *Agriculture: Crop Statistics*; Tables and Interactive Statistical Data for Irrigated and Non-Irrigated Areas; DOS: Amman, Jordan. Available online: https://jorinfo.dos.gov.jo/Databank/pxweb/en/DOS_Database/START__08/AGR_AREA/ (accessed on 16 September 2022).
62. Al-Bakri, J.T. Remote Sensing Techniques for Environmental Monitoring of the Semiarid Zone of Jordan. Ph.D. Thesis, Cranfield University, Bedford, UK, 2000.
63. Al-Bakri, J.T.; Taylor, J.C.; Brewer, T.R. Monitoring land use change in the Badia transition zone in Jordan using aerial photography and satellite imagery. *Geogr. J.* **2001**, *167*, 248–262. [CrossRef]
64. Al-Bakri, J.T. *Crop Mapping and Validation of ALEXI-ET in Azraq and Mafraq Areas*; A Report for Regional Coordination on Improved Water Resources Management and Capacity Building; Ministry of Water and Irrigation: Amman, Jordan, 2015; pp. 19–31.
65. Moriasi, D.N.; Arnold, J.G.; Van Liew, M.W.; Bingner, R.L.; Harmel, R.D.; Veith, T.L. Model evaluation guidelines for systematic quantification of accuracy in watershed simulations. *Trans. ASABE* **2007**, *50*, 885–900. [CrossRef]
66. Burgan, H.I.; Aksoy, H. Daily flow duration curve model for ungauged intermittent subbasins of gauged rivers. *J. Hydrol.* **2022**, *604*, 127249. [CrossRef]
67. Bolstad, P. *GIS Fundamentals: A First Text on Geographic Information Systems*, 6th ed.; Eider Press: White Bear Lake, MN, USA, 2019; p. 764.
68. Mitchell, A. *The Esri Guide to GIS Analysis, Volume 1: Geographic Patterns and Relationships*, 2nd ed.; ESRI Press: Redlands, California, 2020; pp. 105–133.
69. GIZ (German Society for International Cooperation). *Assessment of Surface Water Production, Conveyance and Use in All Sectors in Jordan*; Final Report for Third National Water Master Plan (NWMP-3); GIZ: Amman, Jordan, 2021.
70. Franceschini, G.; De Leo, E.; Muchoney, D. *Jordan—Land Cover Atlas*; FAO: Rome, Italy, 2019; p. 66. Available online: https://www.fao.org/3/ca3388en/CA3388EN.pdf (accessed on 22 October 2022).
71. Kamble, B.; Kilic, A.; Hubbard, K. Estimating Crop Coefficients Using Remote Sensing-Based Vegetation Index. *Remote Sens.* **2013**, *5*, 1588–1602. [CrossRef]
72. Hunsaker, D.J.; Pinter, P.J., Jr.; Kimball, B.A. Wheat basal crop coefficients determined by normalized difference vegetation index. *Irrig. Sci* **2005**, *24*, 1–14. [CrossRef]
73. Reyes-González, A.; Trooien, T.; Kjaersgaard, J.; Hay, C.; Reta-Sánchez, D.G. Development of Crop Coefficients Using Remote Sensing-Based Vegetation Index and Growing Degree Days. In Proceedings of the ASABE Annual International Meeting, ASABE Paper No. 162462560, Orlando, FL, USA, 17–20 July 2016. [CrossRef]

74. Margane, A.; Qadi, M.; Kurdi, O. *Updating the Groundwater Contour Map of the A7/B2 Aquifer in North Jordan*; Technical Report prepared by BGR Project Syrian Refugee Response 2009.2209.6, BGR archive no. 0132576; BGR and GIZ: Amman, Jordan, 2015; p. 130.
75. Shatanawi, M.; Fardous, A.; Mazahrih, N.; Duqqah, M. Irrigation systems performance in Jordan. In *Irrigation Systems Performance*; Lamaddalena, N., Lebdi, F., Todorovic, M., Bogliotti, C., Eds.; (Options Méditerranéennes: Série B. Etudes et, Recherches; n., 52); CIHEAM: Bari, Italy, 2005; pp. 123–131.
76. MWI and BGR (Ministry of Water and Irrigation; Bundesanstalt für Geowissenschaften und Rohstoffe). *Groundwater Resource Assessment of Jordan*; MWI and BGR: Amman, Jordan, 2019.
77. MWI (Ministry of Water and Irrigation, Jordan). *Jordan's Water Strategy 2016–2025*; Ministry of Water and Irrigation: Amman, Jordan, 2016.
78. Saidan, M.N.; Al-Addous, M.; Al-Weshah, R.A.; Obada, I.; Alkasrawi, M.; Barbana, N. Wastewater Reclamation in Major Jordanian Industries: A Viable Component of a Circular Economy. *Water* **2020**, *12*, 1276. [CrossRef]
79. GIZ & MWI. *Third National Water Master Plan (NWMP-3), Volume B—Water Resources*; Technical Report; Management of Water Resources Project: Jordan, Amman, 2022; p. 181.